DIGITAL CONTROL OF GYROSCOPE DRIFT COMPENSATION

by

Donald W. Fleischer

B. E. E., Union College

1956

SUBMITTED IN PARTIAL FULFILLMENT OF THE

REQUIREMENTS FOR THE DEGREE OF

MASTER OF SCIENCE

at the

MASSACHUSETTS INSTITUTE OF TECHNOLOGY

June, 1961

Signature of Author_____
Department of Electrical Engineering, May 20, 1961

Certified by_____
Thesis Supervisor

Accepted by_____
Chairman, Departmental Committee on Graduate Students

DIGITAL CONTROL OF GYROSCOPE DRIFT COMPENSATION

by

Donald W. Fleischer

Submitted to the Department of Electrical Engineering on May 20, 1961 in partial fulfillment of the requirements for the degree of Master of Science.

ABSTRACT

This thesis is concerned with the use of digital signals for the control of gyroscope drift compensation. Several possible methods for digitally controlling the torque produced by a gyroscope torque generator are presented with block diagrams of the hardware required. Possible sources of error introduced by the use of these methods are analyzed. Tests that were conducted using the torque control methods presented are described. The results indicate that digitally controlled gyroscope drift compensation is quite feasible if certain requirements are followed.

Thesis Supervisor: Richard H. Frazier

Title: Associate Professor of Electrical Engineering

E E.

Plant

1961

ACKNOWLEDGEMENT

The author is grateful to Professor Richard Frazier for his supervision and assistance in acting as thesis adviser.

The author wishes to thank those personnel of the M. I. T. Instrumentation Laboratory who assisted with their comments and especially Harry Margulius who worked with the author during many of the tests.

The author also wishes to thank his wife for her efforts and patience in typing this thesis.

This report was prepared under Project 52-154, Division of Sponsored Research, Massachusetts Institute of Technology, sponsored by the Navigation and Guidance Laboratory of the Wright Air Development Division, Department of the Air Force, under Contract AF33(600) - 38967.

TABLE OF CONTENTS

TABLE OF CONTENTS (continued)

LIST OF FIGURES

INTRODUCTION

With the advent of the replacement of analog computers by special purpose digital computers in inertial navigation systems, certain changes in the system instrumentation have become necessary. One of these required changes is in the method used to compensate for gyroscope drift. Basically, the problem is one of using sampled data to perform a function where continuous signals were previously available.

Gyroscope drift is caused by unwanted torques which act on the gyroscope torque summing member about the output axis. These unwanted torques result from inaccuracies in the manufacture of the gyroscope and from certain causes inherent in its design. Ideally, a drift compensation system applies a torque to the gyroscope float which occurs simultaneously with and is equal in magnitude and opposite in direction to the unwanted torques, thus completely cancelling them.

Some of the unwanted torques are functions of gravity and the acceleration of the vehicle in which the inertial navigation system is contained. When a gyroscope is mounted in an inertial system, there is no way of distinguishing between these torques and the desired precession torques. Therefore, before the gyroscope is mounted in the system, the magnitudes and directions of the unwanted torques must be determined for conditions of gravity and acceleration which the vehicle will encounter. One of the functions of the inertial system computer is to take this previously determined information and

calculate, for existing conditions, what the unwanted torques are and hence what the compensating torques should be.

When an analog computer is used for this function, continuous torque information is produced. In this form, the information is ideally suited to controlling compensating torques, since the unwanted torques are continuous quantities. Thus a compensation system employing analog computation is theoretically capable of producing ideal compensation.

Digital computers, due to their nature, produce discontinuous output information. Therefore a compensation system employing digital computation, even under ideal conditions, cannot achieve ideal compensation. This means that unwanted torques act on the gyroscope float causing small angular movements. These movements can be the source of certain errors. This thesis investigates some possible digital compensation methods and attempts to analyze the errors introduced by them.

The first chapter briefly reviews the causes of gyroscope drift. It gives the equation that describes the unwanted torques causing the drift and tells how the constants are obtained. Gyroscope torque generator operation and analog drift compensation are also outlined.

Chapter II gives descriptions of several possible methods of instrumenting a digital compensation system. It lists the advantages and disadvantages of each method.

Chapter III analyzes the errors introduced by the compensation methods of Chapter II.

The fourth chapter describes tests that were made on a gyroscope to determine the actual errors introduced by digital controlled compensation. A description is given of the equipment used and the results are presented.

The last chapter briefly analyzes the results of Chapter IV. Some conclusions are drawn and a short summary given.

Chapter I

GYROSCOPE DRIFT

1.1 The Gyroscope

The gyroscopes referred to in this thesis are of a particular type, namely floated single-degree-of-freedom integrating gyroscopes of the type designed and built by the M. I. T. Instrumentation Laboratory. No detailed explanation of these units or their operation will be given here since this is more than adequately covered by existing literature, including references (2,3). Figure 1-1, however, which is a line schematic of the gyroscope showing its essential components and axes, is supplied for convenience. The torque summing member of the gyroscope, referred to later, consists of the float, which contains the gyro wheel and gimbal structure, the torque generator rotor, signal generator rotor and connecting shaft.

Since the compensating torques are applied to the gyroscope torque summing member by the torque generator, a short explanation of this component is now given. The torque generator type used extensively in Instrumentation Laboratory gyroscopes is the Microsyn. It is a variable reluctance electromagnetic torque motor with a special two-pole rotor and four-pole stator. The stator is wound with either one or two windings, while the rotor has no windings. Only the two winding type is considered here.

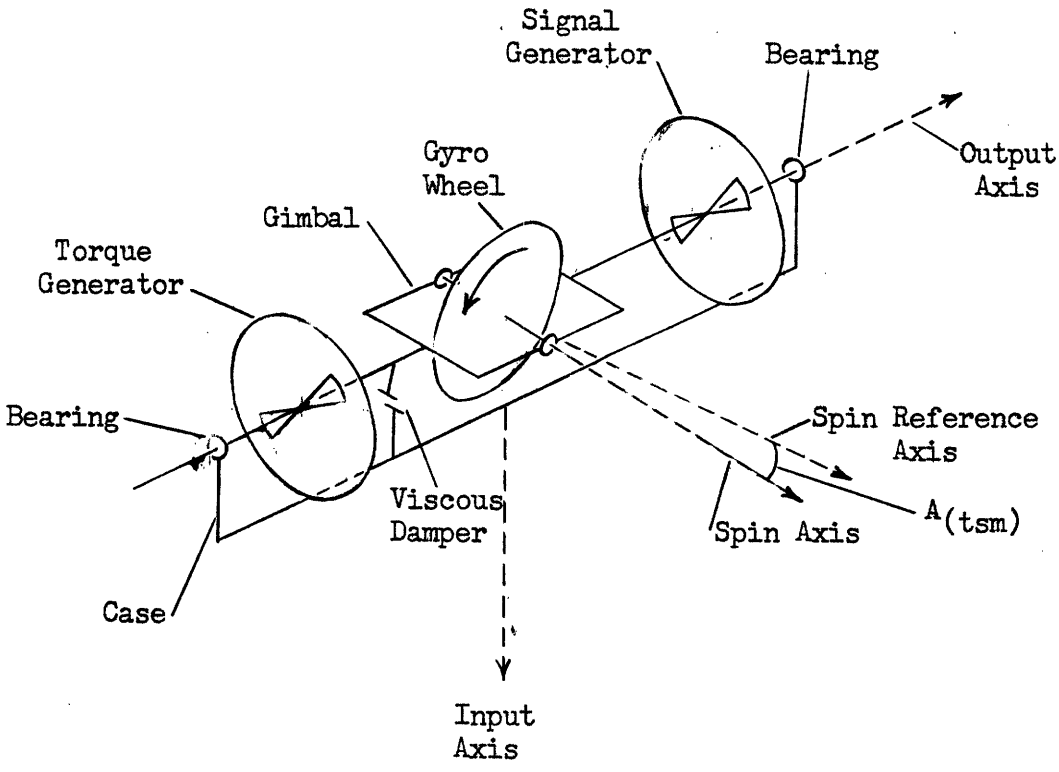

Figure 1-1 Line Schematic Diagram
of Gyroscope

The torque produced by the torque generator is proportional to the product of the currents applied to the two windings. These may both be direct currents or both alternating currents. The direction of the torque produced depends on the polarity or phase of the currents applied to the two windings. In this thesis, the torque produced will be considered positive if both currents have the same polarity or are in phase and negative if they are of opposite polarity or 180° out of phase, using the same terminal connections in all cases.

In use, a current of constant magnitude or amplitude is generally applied to one winding, called the excitation winding, while the current to the second or input winding is varied. The torque then becomes proportional to the input current. The equation describing the torque produced by the torque generator is:

$$M_{(tg)} = S_{(tg)} i_{(ex)(tg)} i_{(in)(tg)} \qquad (1\text{-}1)$$

where

$M_{(tg)}$ = torque generator output torque

$S_{(tg)}$ = torque generator sensitivity

$i_{(ex)(tg)}$ = torque generator excitation current

$i_{(in)(tg)}$ = torque generator input current

If alternating currents of the same frequency are used, the average or effective torque produced is:

$$M_{(tg)} = 1/2\ S_{(tg)} I_{(ex)(tg)} I_{(in)(tg)} \cos \phi \qquad (1\text{-}2)$$

where

$I_{(ex)(tg)}$ and $I_{(in)(tg)}$ = the amplitudes of the torque generator currents

ϕ = phase angle between the two currents

Therefore when the two currents are 90° out of phase the effective torque produced is zero. The torque is independent of frequency over a specified operating range. In this thesis, any torques referred to will be effective torques, unless otherwise specified.

1.2 Causes of Inaccuracy Torques

Essentially there are four types of torques that operate on the gyroscope torque summing member. They are: (a) the gyro wheel precessional torque caused by an angular velocity of the gyroscope case with respect to inertial space about the input axis; (b) the viscous damping torque; (c) desired torques produced by the torque generator and (d) inaccuracy torques. The first three are considered to be perfect torques. In actual operation the torques usually grouped under these headings are not perfect. However, here they each are considered to be separated into perfect and imperfect parts, the latter parts all being included with the inaccuracy torques. If the inaccuracy torques, also referred to as unbalance torques or drift torques, were not present, the gyroscope would perform perfectly.

The inaccuracy torques can be further divided into error torques and uncertainty torques. Error torques are by definition predictable

and therefore can be compensated. Uncertainty torques are unpredictable and hence cannot be compensated. Assuming the error torques can be perfectly predicted and compensated, the ultimate gyroscope performance limit is determined by the magnitude of the uncertainty torques.

Inaccuracy torques are caused by several factors. The significant ones are listed below. The following abbreviations are used during this discussion:

S. R. A. = spin reference axis

I. A. = input axis

O. A. = output axis

(a) Fixed unbalance or pendulous torques, caused by the center of mass of the torque summing member not lying exactly on the gyroscope output axis. For analysis, the unbalance is separated into two components, one assumed fixed along the positive S. R. A., $U_{(SRA)}$, and one assumed fixed along the positive I. A., $U_{(IA)}$, both measured in gram-cm. These unbalance components are reduced as much as possible by balancing nuts along each of the axes.

(b) Compliance torques, caused by the torque summing member not having equal compliances in all directions. The compliances that contribute to these torques are:

$K_{(SS)}$ = the compliance along S. R. A. due to a force acting along S. R. A.

$K_{(SI)}$ = the compliance along S. R. A. due to a force acting along I. A.

$K_{(SO)}$ = the compliance along S. R. A. due to a force acting along O. A.

$K_{(IS)}$ = the compliance along I. A. due to a force acting along S. R. A.

$K_{(II)}$ = the compliance along I. A. due to a force acting along I. A.

$K_{(IO)}$ = the compliance along I. A. due to a force acting along O. A.

The units of these compliances are cm/dyne.

Figure 1-2 shows how unequal compliances can cause unwanted torques to act on the torque summing member. Only the two compliances $K_{(SS)}$ and $K_{(II)}$ are considered here. The mass reaction force F, acting on the center of mass, is due to gravity and any acceleration of the gyroscope case, i. e., $F = \bar{g} - \bar{a}$. The units of F are cm/sec^2. The components of F along S. R. A., $F_{(SRA)}$, and I. A., $F_{(IA)}$, acting on the unequal compliances $K_{(SS)}$ and $K_{(II)}$ cause the center of mass to be displaced along the line OB. F then no longer acts through the output axis, but on the lever arm OC, causing a torque about the output axis.

(c) Buoyancy torques, caused by the center of buoyancy of the torque summing member not lying on the output axis. In practice it is difficult to distinguish between these torques and fixed unbalance torques, since they both have the same effects. Therefore the constants $U_{(SRA)}$ and $U_{(IA)}$ include buoyancy unbalances.

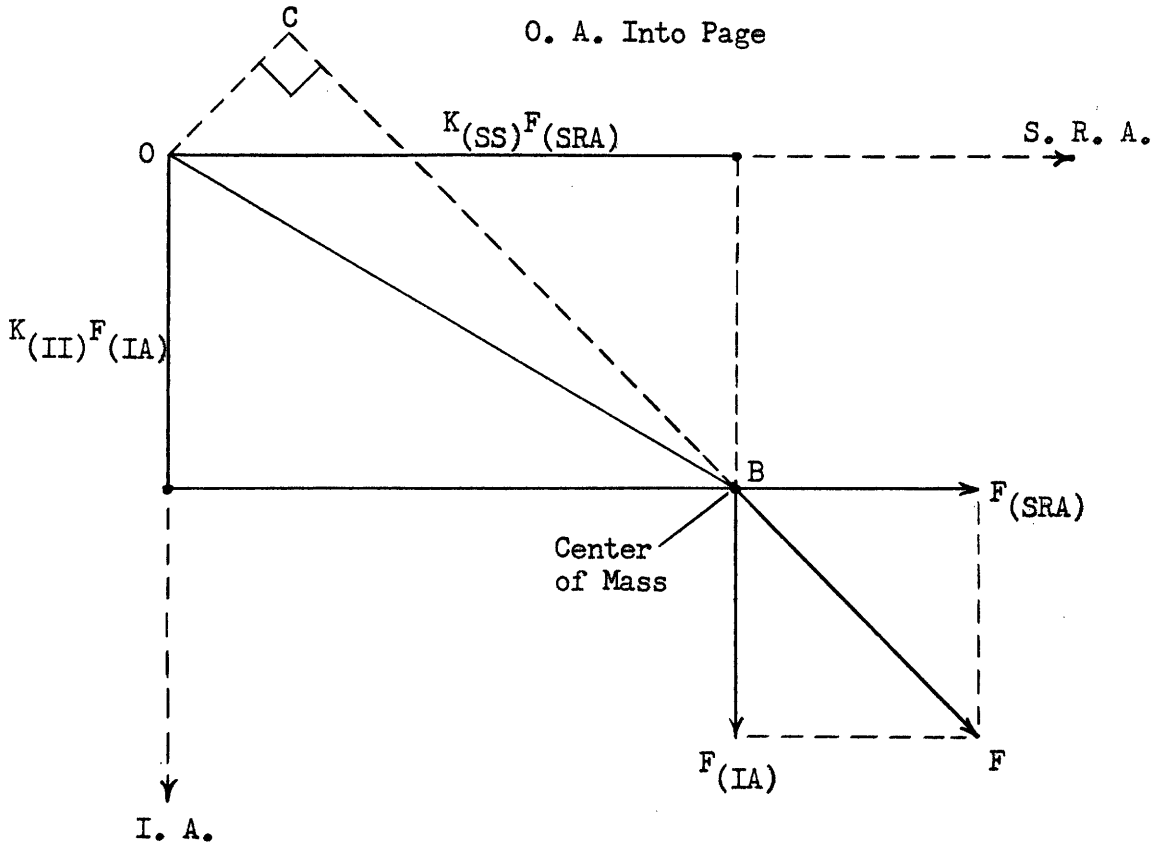

Figure 1-2 Diagram Showing How Unequal Compliances Can Cause Inaccuracy Torques

(d) Power lead torques, caused by electrical connections to the torque summing member. Since the power leads are constructed to behave like springs, the torques they produce have a gradient proportional to the angular deviation of the torque summing member from null, as well as a constant part at null.

(e) Signal generator reaction torque, caused in part by secondary loading which makes the signal generator behave like a torque generator. Since the secondary current is proportional to the angular deviation from null, the torque produced has properties similar to power lead torques, exhibiting a bias at null and an angular dependent part.

(f) Torque generator reaction torque, caused by certain non-symmetries in the Microsyn. This torque varies with the square of the excitation current and also with the angular deviation from null.

(g) Hydrodynamic torques, caused by movements, other than rotational, of the gyroscope float relative to the case.

(h) Convection torques, caused by temperature variations throughout the damping fluid.

(i) Friction torque in the torque summing member jewel and pivot suspension. This torque is effected greatly by the load placed on the suspension, which depends upon the difference in mass of the torque summing member and the damping fluid displaced by the float, as well as F.

1.3 Error Torque Equation

Uncertainty torques are unpredictable not only as to their magnitudes, but in many instances also their origins. Thus, in several cases the above mentioned torques contribute to both the error and uncertainty torques. Torques 1.2 (g), (h) and (i) are, for the most part, uncertainty torques. Therefore the error torques are usually considered to be composed of those described in 1.2 (a) through (f). The equation describing these torques is now derived.

Torques 1.2 (a), (b) and (c) are dependent upon the specific force acting on the gyroscope. The force F is resolved into components lying along S. R. A., I. A. and O. A. These force components are considered positive when they are directed along these axes in the positive directions as determined by the arrows of Figure 1-1. Unbalances and compliance deflections are considered positive if they lie along the positive axes.

Referring to Figure 1-1, the two unbalances considered give rise to the torque about O. A.:

$$U_{(SRA)}F_{(IA)} - U_{(IA)}F_{(SRA)} \qquad (1\text{-}3)$$

The torque about O. A. due to unequal compliances is obtained by referring to Figure 1-2. The deflections due to only two of the compliances considered in 1.2 (b) are shown in the diagram, but the same reasoning is easily extended to include the other four. The lever arm produced by the deflection $K_{(SS)}F_{(SRA)}$ is acted upon by the

force $F_{(IA)}$ and the lever arm $K_{(II)}F_{(IA)}$ is acted upon by $F_{(SRA)}$, producing the torque:

$$K_{(SS)}F_{(SRA)} \cdot F_{(IA)} - K_{(II)}F_{(IA)} \cdot F_{(SRA)} \tag{1-4}$$

Likewise the other four compliances produce the torque:

$$K_{(SI)}F_{(IA)} \cdot F_{(IA)} + K_{(SO)}F_{(OA)} \cdot F_{(IA)}$$
$$- K_{(IS)}F_{(SRA)} \cdot F_{(SRA)} - K_{(IO)}F_{(OA)} \cdot F_{(SRA)} \tag{1-5}$$

Since the gyroscope angular deviation from null is usually very small, only the constant parts of torques 1.2 (d), (e) and (f) are considered. These are grouped into a constant term, R, measured in dyne/cm. The final error torque equation is therefore:

$$M_E = R + U_{(SRA)}F_{(IA)} - U_{(IA)}F_{(SRA)} + \left[K_{(SS)} - K_{(II)}\right] F_{(IA)}F_{(SRA)}$$
$$+ K_{(SI)}F^2_{(IA)} - K_{(IS)}F^2_{(SRA)} + K_{(SO)}F_{(OA)}F_{(IA)}$$
$$- K_{(IO)}F_{(OA)}F_{(SRA)} \tag{1-6}$$

The constants of the above equation are obtained by performing tumbling tests on each gyroscope. Essentially this consists of mounting the gyroscope on a slowly rotating turntable and making a record of the torque required to keep the torque summing member at null, while the gyroscope orientation relative to gravity is continually changing due to the turntable rotation. Thus, in this case $F = \bar{g}$. When the turntable axis is properly oriented, the record obtained yields the error torque as a function of turntable angle. A Fourier analysis of these results yields the constants of equation

(1-6). These tests are covered in great detail in references 1 and 2.

1.4 Analog Drift Compensation

In an analog drift compensation system, the various force components are obtained from linear accelerometers aligned along the three gyroscope input axes, which also correspond to the three major axes of each gyroscope. These force components are represented by various voltage levels. The associated analog computers, one for each gyroscope, are composed of amplifiers, potentiometers and related components. The error constants are put into the computers by setting appropriate potentiometers. Each computer output is a voltage, which is fed to a matching amplifier. The output of the matching amplifier goes to the torque generator input winding of the associated gyroscope.

In many cases, to simplify equipment, not all of the terms of equation (1-6) are calculated. Some of the compliance terms are found to contribute only a small amount to gyroscope drift and these may be eliminated.

Chapter II

DIGITAL DRIFT COMPENSATION METHODS

2.1 System Computer

In a digital drift compensation system the compensation torque required for each gyroscope is calculated by a digital computer. Many possibilities exist as to the type of digital computer to be used and the form that the computer output takes. The intention of this thesis is not to determine the type of computer to be used. This is determined by the requirements of the rest of the inertial system. Therefore a general type of digital computer is assumed to be used that operates in the following manner. Periodically sampled digital specific force data from the inertial system accelerometers are fed into the computer. By using this data and the required gyroscope error constants stored in its memory, the computer calculates the compensation torque magnitude from equation (1-6). The compensation torque direction is opposite that of (1-6). This is read out in parallel form as a binary number whose magnitude is equal to the torque magnitude and one digit of which represents the torque direction. The number of digits in the binary number depends upon the accuracy desired. The rate at which new torque calculations are made depends upon how closely changes in the error torque need to be followed. While the output can take other forms, depending on the type computer

used, all these forms can be easily changed to the form described above.

2.2 Torque Control Methods

This chapter considers methods by which the digital computer output can be directly used to control the compensation torque applied to the gyroscope torque summing member. Essentially the problem is one of using digital signals to control the input current to a gyroscope torque generator. Three ways torque generator input current can be controlled in order to vary the effective torque output are: (1) the level of the input current can be varied; (2) if alternating currents are applied to the input and excitation windings, the phase angle between the two currents can be varied, while keeping the amplitudes constant; and (3) the application time of a periodically applied, constant amplitude input current can be varied.

The first two ways mentioned above are based on the normal operation of the Microsyn, described in Chapter 1. The third way is based on the integrating properties of the gyroscope. Neglecting, for the moment, the effects of a stabilization servo drive, integration as performed by the gyroscope float is described by the equation:

$$\Delta A_{(tsm)} = \frac{1}{C_d} \int_0^t M_{(tsm)}\, dt \qquad (2\text{-}1)$$

where

$\Delta A_{(tsm)}$ = angle of rotation of torque summing member

C_d = damping coefficient of gyroscope float

$M_{(tsm)}$ = forcing torque acting on the torque summing member

Only two torques acting on the torque summing member are considered here, the error torque and compensation torque. Thus, the precessional torque and any command torques applied through the torque generator are omitted, since their presence does not effect the problem. Also uncertainty torques are omitted, since their presence cannot be predicted. Equation (2-1) then becomes:

$$\Delta A_{(tsm)} = \frac{1}{C_d}\left[\int_0^t M_E\,dt + \int_0^t M_C\,dt\right] \qquad (2\text{-}2)$$

where

M_C = compensation torque

Therefore, in order that there be no net angular deviation of the torque summing member due to error torques occurring during the time interval $0 \rightarrow t$, it is sufficient that:

$$\int_0^t M_E\,dt = -\int_0^t M_C\,dt \qquad (2\text{-}3)$$

In this case $\Delta A_{(tsm)}$ will not necessarily be zero during the whole time interval, since this would require: $M_E(t) = -M_C(t)$. Also $\Delta A_{(tsm)}$ willnot necessarily be zero at time t, since the final position of the torque summing member is approached assymptotically at a rate depending on the time constant of the gyroscope.

2.3 Instrumenting Torque Control Methods

Method 1 - A block diagram of one way of digitally changing the input current level to the torque generator is shown in Figure 2-1. Various voltage levels are produced by a voltage divider, if direct current is used, or a tapped transformer, if alternating current is used. Each level is controlled by an electronic switch. The torque magnitude determined by the computer is read into the flip flop register at the beginning of each time interval. Through appropriate AND circuits the flip flops control which level switch is activated. The direction or phase of the input current is controlled by the torque direction flip flop and the reversing switch.

The electronic switches are turned on and off by appropriate voltage levels applied to their control terminals. The flip flop outputs are voltage levels, while their inputs are pulses. Figure 2-1 shows only three different current levels plus zero current. However, this method can be extended to as many levels as desired, depending upon the number of digits used to express the torque magnitude.

Since this method can produce several continuous torque levels, the error torque can be closely approximated, almost eliminating float movements due to the differences between the magnitudes of M_E and M_C. However, the equipment becomes more complex as more torque levels are added in order to obtain a closer torque approximation.

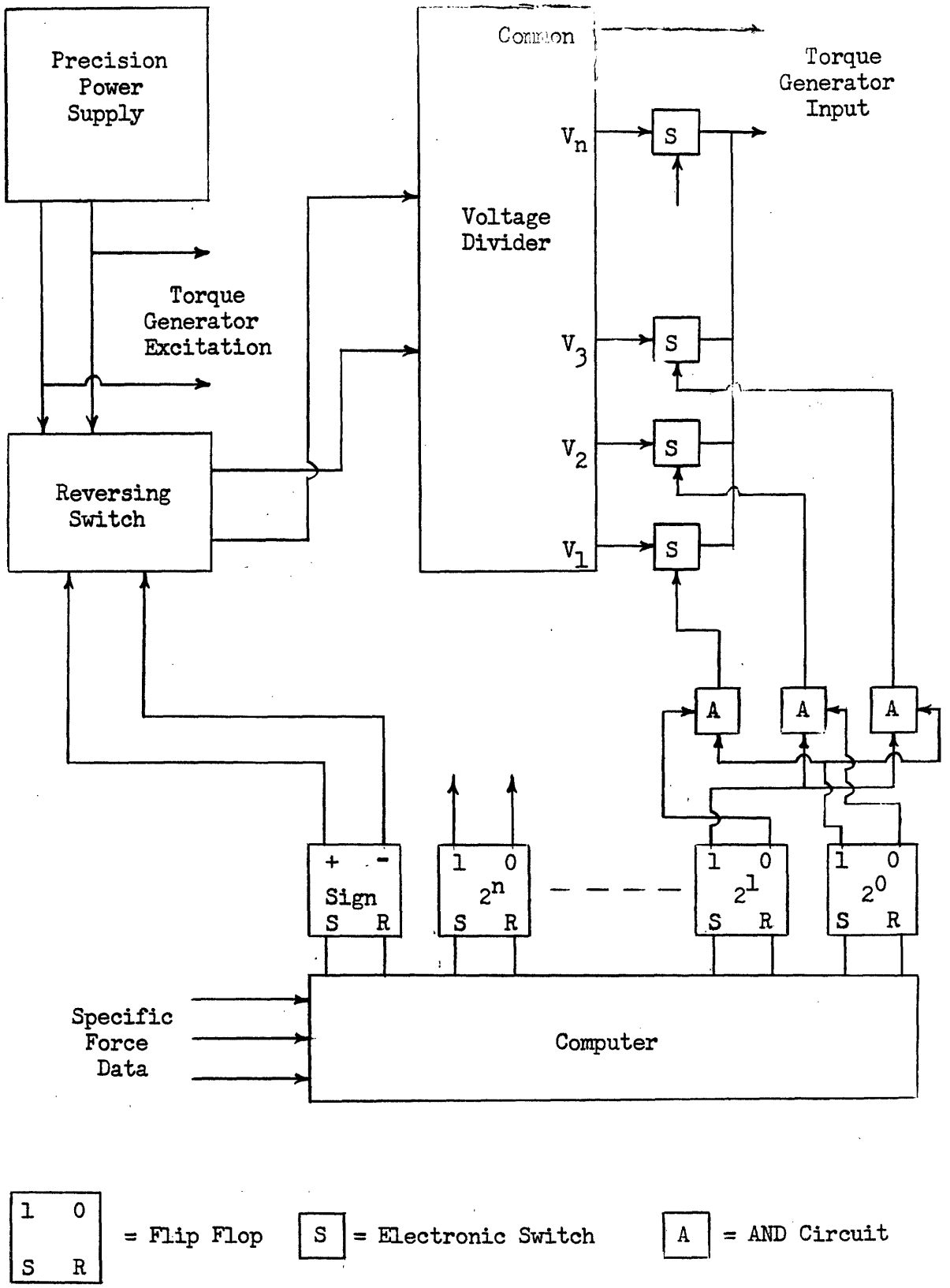

Figure 2-1
Block Diagram of Torque Control Method #1

Method 2 - Another method of controlling the torque is shown in Figure 2-2. For the condition of zero net output torque, the switch flip flop changes state once every clock pulse and controls an electronic switch which changes the direction or the phase of the input winding current. Thus, the torque is constantly changing direction at clock rate. The inhibit circuit blocks a clock pulse from passing through it to the switch flip flop whenever a coincident pulse appears at its other input. At the start of each time interval, the compensation torque is read from the computer into the countdown register and sign bit flip flop. Clock pulses then cause the register to count down to zero. Each time the register counts down one digit a clock pulse is allowed to pass to the inhibit circuit, blocking a clock pulse from the switch flip flop. When the register reaches zero, no more pulses can pass to the inhibit circuit. Thus, the switch flip flop remains in its last state as long as the register is counting down. The sign bit flip flop controls which state the switch flip flop is in when the countdown register starts. The state that the switch flip flop is in and the length of time it stays there determine the direction and magnitude of the net torque. Figure 2-3 is a diagram of the countdown register. Time delays are assumed to be zero in the diagrams presented here.

The torque magnitude produced by the torque generator with the switch flip flop continuously in one state, $M_{(out)(max)}$, must be greater than the maximum expected error torque. Also, $M_{(out)(max)} \cdot \frac{1}{k}$

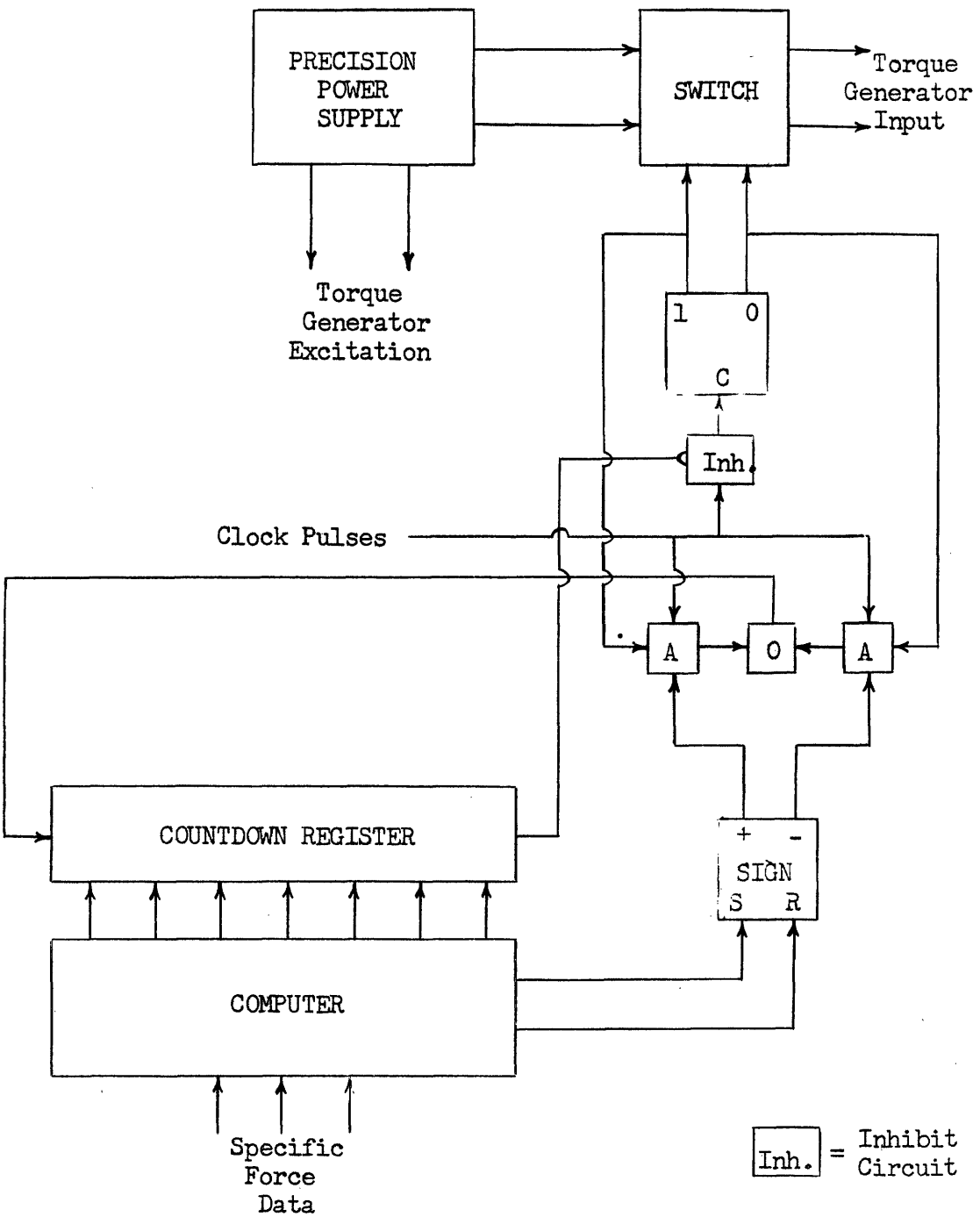

Figure 2-2 Block Diagram of Torque Control Method #2

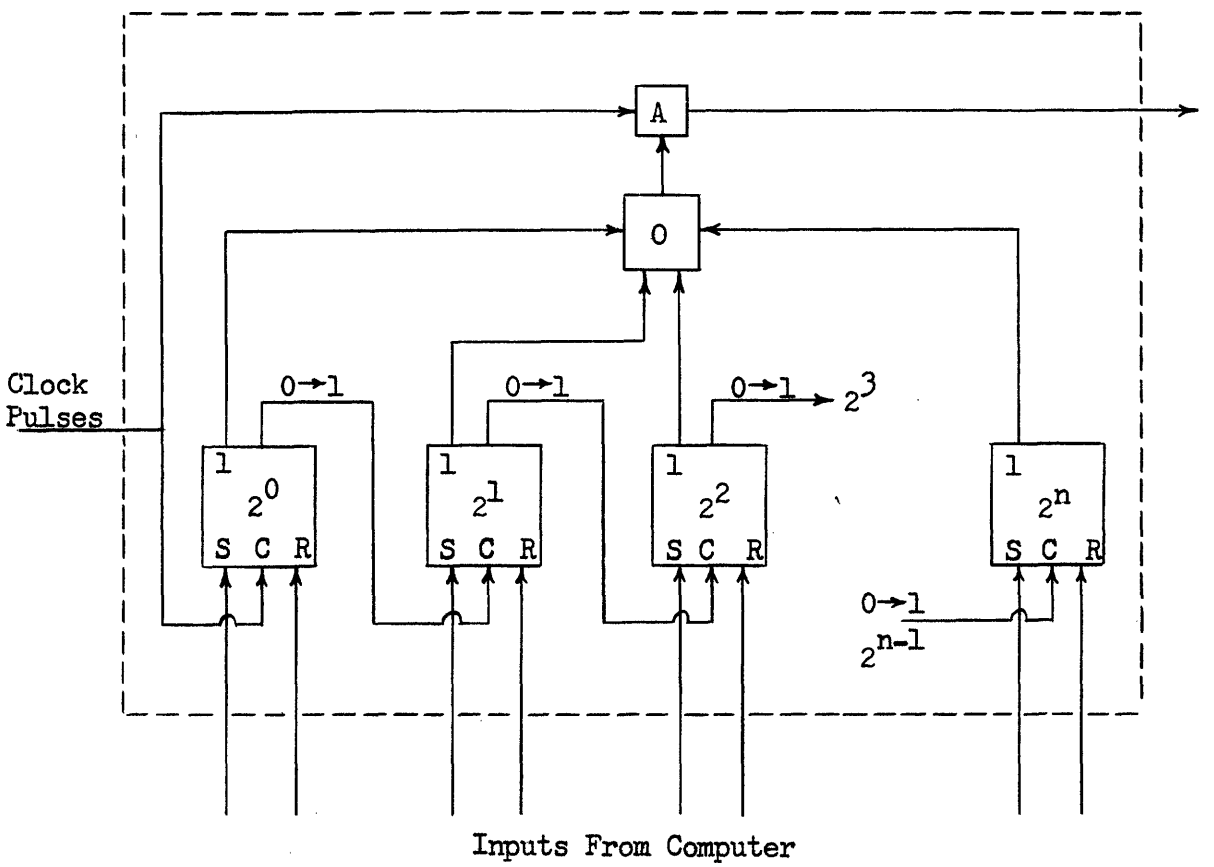

Figure 2-3 Block Diagram of Countdown Register

must equal one digit in the least significant column of the computed compensation torque, where k is the number of clock pulses per computation interval.

Either direct or alternating current can be used on the two torque generator windings. If alternating current is used, the clock pulses must be synchronized at some multiple of the current frequency. Also they must occur when the torque generator input voltage is at the proper phase angle. Figure 2-4 shows the ideal current waveforms for zero torque, using direct current in part (a) and alternating current in part (b). For part (b), the clock rate is one pulse per cycle.

This method has the advantage of requiring a minimum amount of equipment. Also the I^2R loss in the torque generator windings is constant, thus minimizing resistance variations due to heating. The disadvantage of this method is that if the torque magnitude is not exactly the same in each direction, then a desired zero torque will actually have some finite value. Under conditions of low specific force, the compensation torque required will be zero for a large part of each interval. Therefore the error will have a longer time to accumulate than for a method in which no torque generator input current flows for a desired zero torque output.

Method 3 - Another way of controlling the torque is to have one torque magnitude which is on in either direction or is off. A block diagram of one way of instrumenting this appears in Figure 2-5.

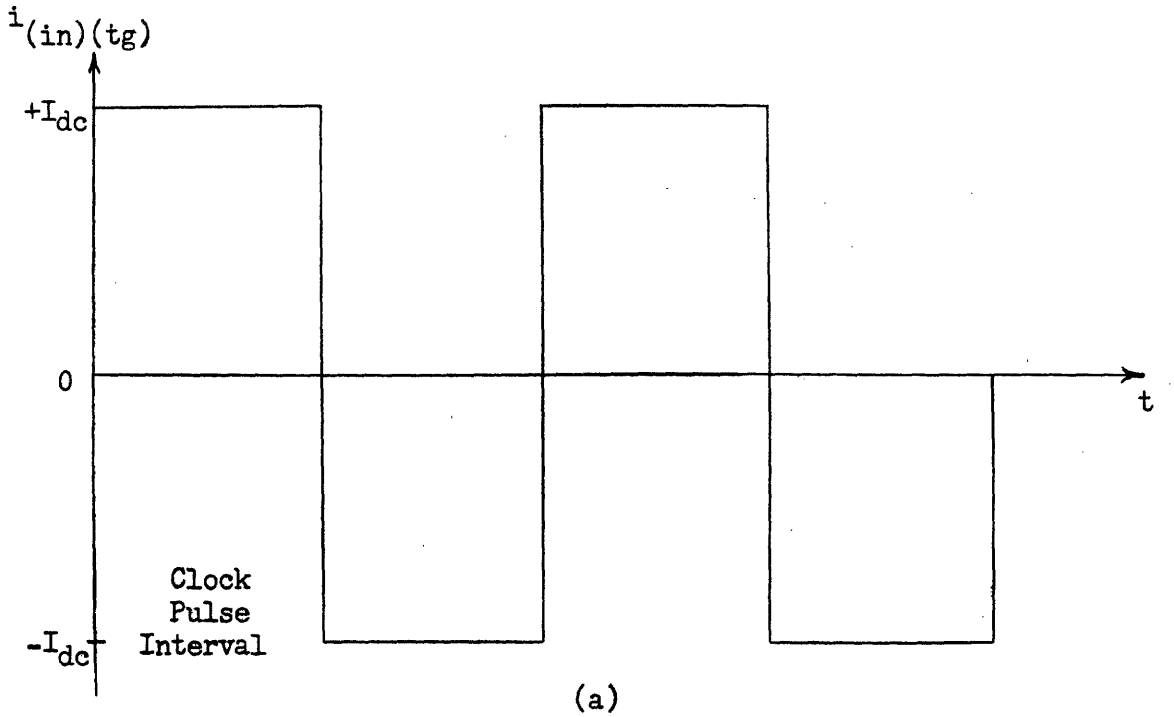

(a)

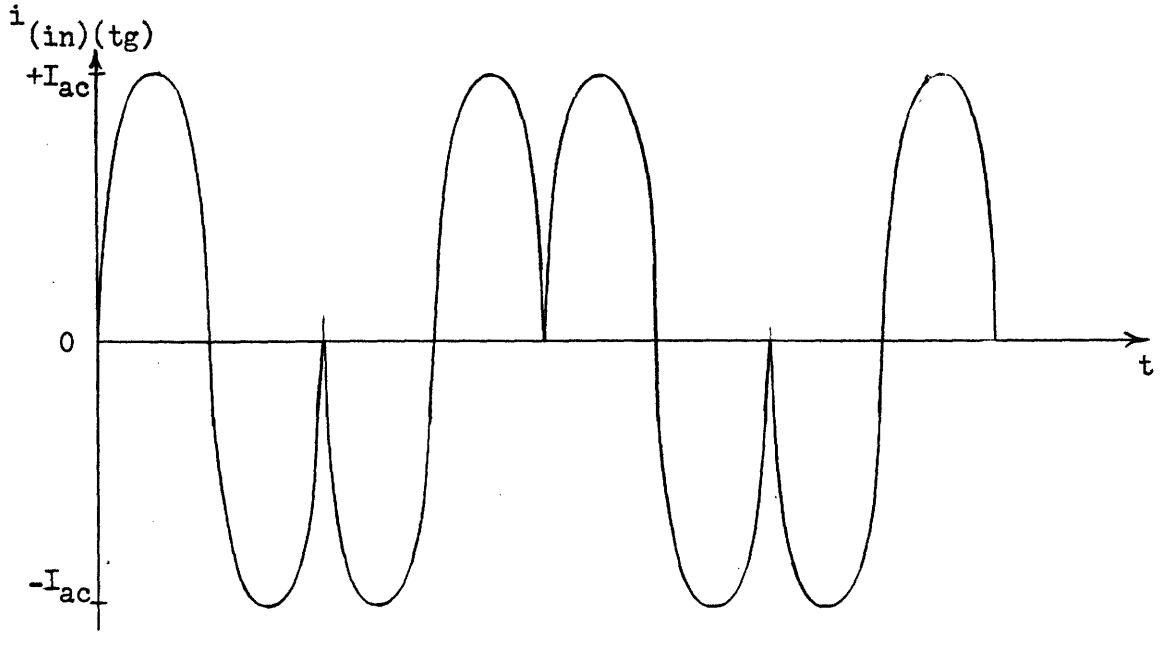

(b)

Figure 2-4 Ideal Current Waveforms for Zero Torque Output Using Torque Control Method #2

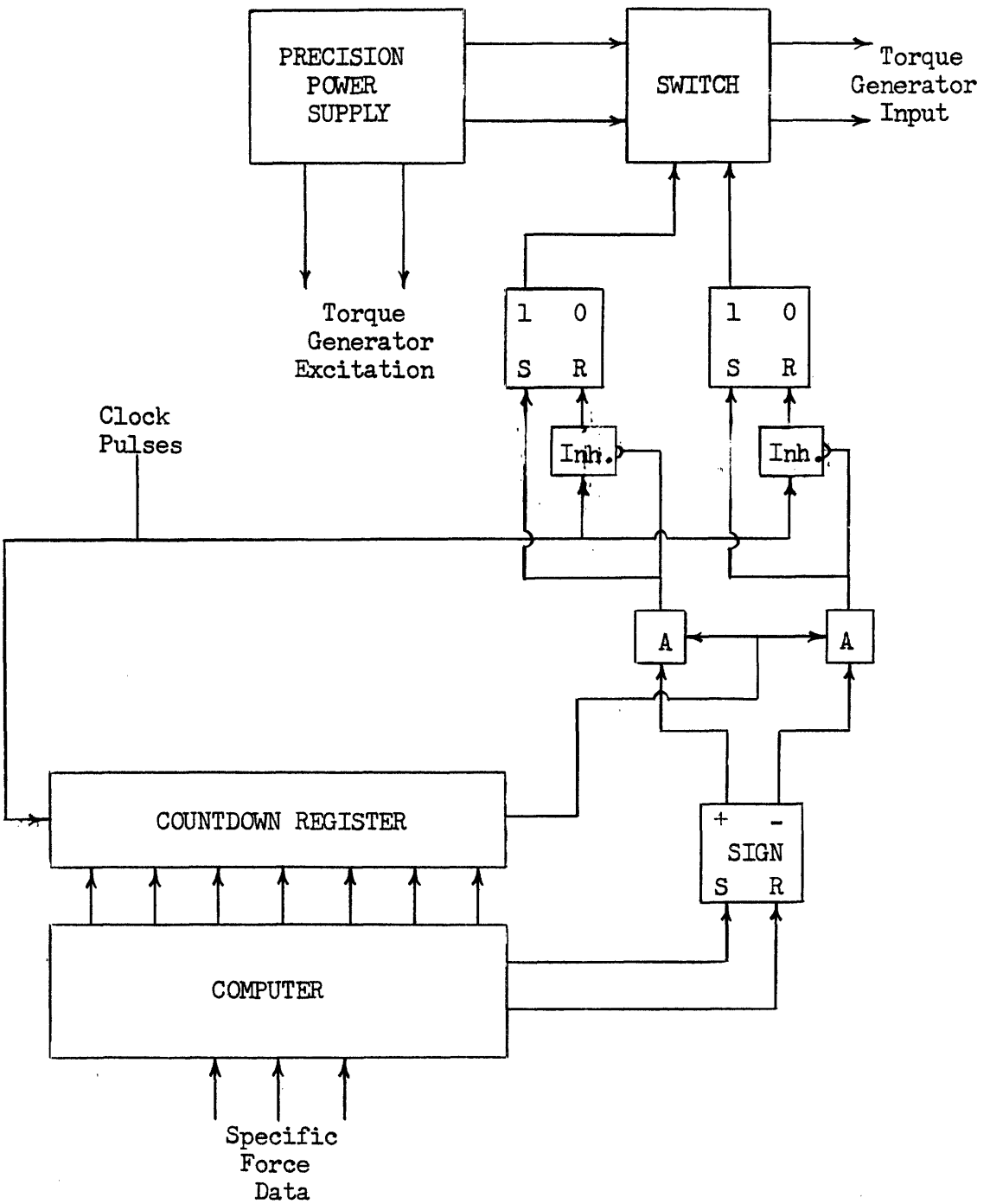

Figure 2-5 Block Diagram of Torque Control Method #3

As in the previously desribed method, the computer reads the torque into the countdown register and sign bit flip flop at the start of each time interval. Normally the two switch flip flops are kept in the zero position by clock pulses appearing at the reset inputs. When the register starts counting down, clock pulses are allowed to appear at the set input of one of the flip flops, while blocking the pulses from the reset input through the inhibit circuit. The sign bit flip flop determines which of the two switch flip flops the pulses set. After the countdown register reaches zero, the clock pulses again appear at the reset inputs of both flip flops. Thus, for a torque other than zero, the switch is on in one direction for a certain amount of time at the start of each interval and then off for the rest of the interval.

This method has the advantages of being simple to instrument and of producing exactly zero torque when this condition is desired. As in method 2, the input current level to the electronic switch is such that $M_{(out)(max)} \cdot \frac{1}{k}$ = least significant digit of computed torque.

Method 4 - The previous two methods for controlling the torque depend completely upon the integration action of the gyroscope float for the time integration of the individual error torque computations. That is, as soon as the required compensation torque is calculated by the computer, it is applied to the gyroscope. Another method is to integrate the torque digitally over a period of time until a point

is reached when the compensation torque required is equal to the single torque magnitude available. Then applying this torque magnitude for one time interval cancels out the total effects the error torque has caused over several intervals.

Figure 2-6 shows the block diagram of one way of instrumenting such a method. Once each interval, the required compensation torque is calculated by the computer and the result fed into the reversible adder. This continues each interval until the capacity of the adder is exceeded. At that point, the adder generates a carry-out pulse to set one of the switch flip flops. At the end of the interval, the switch flip flop is reset by a pulse from the computer. The binary number contained in the adder represents the compensation torque magnitude that, applied for one time interval, brings the gyroscope torque summing member back to null. Thus, the torque magnitude that is actually applied to the torque summing member should be one torque unit larger than the capacity of the adder.

This method has the advantage of obtaining perfect integration of the computed torque during the time that the digital adder is performing the integration. A disadvantage is that the angular deviations of the gyroscope float are larger, since the compensation torque is applied at less frequent intervals.

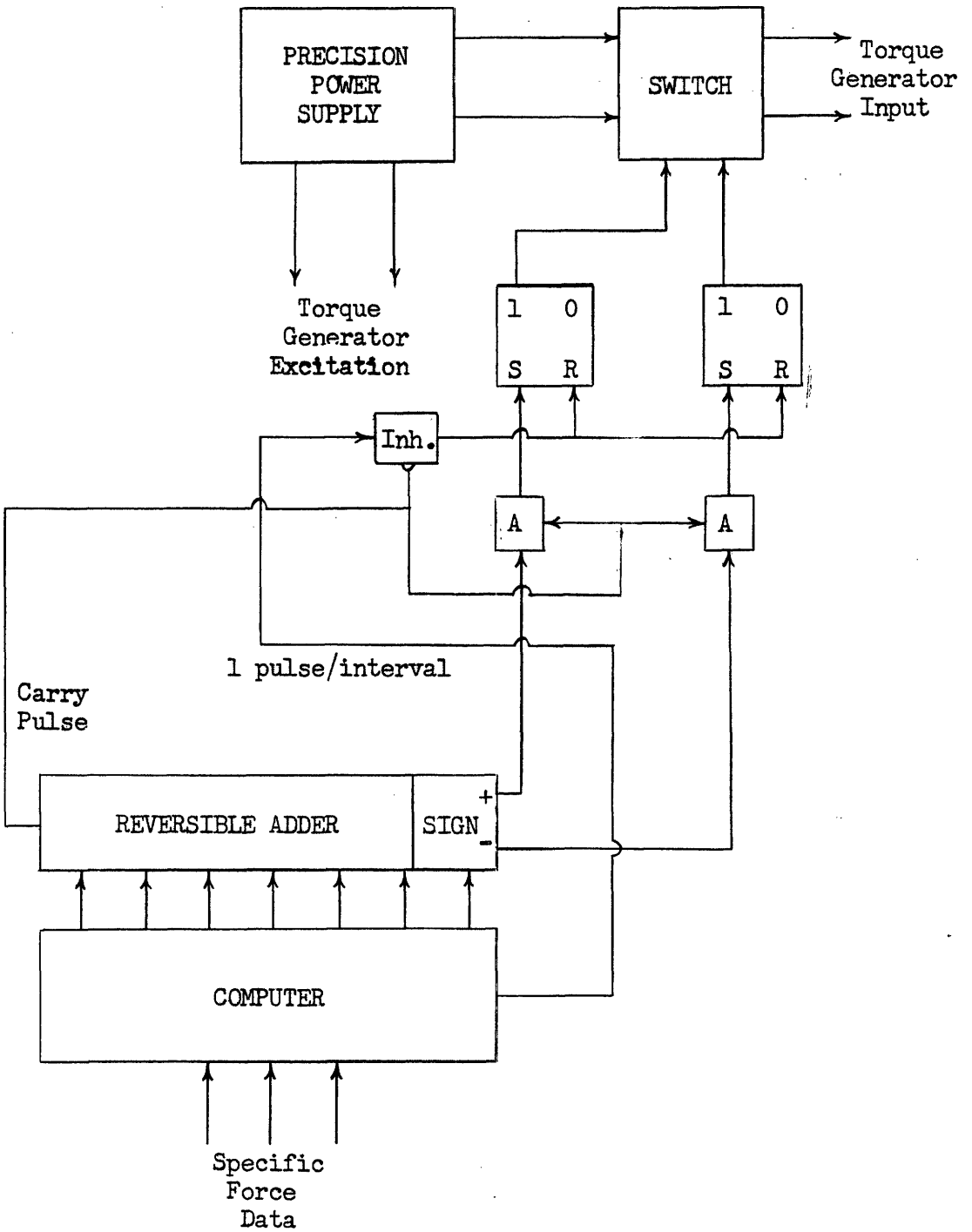

Figure 2-6 Block Diagram of Torque Control Method #4

Chapter III

DEVIATIONS OF DIGITAL COMPENSATION FROM THE IDEAL

3.1 Introduction

In Chapter II, digital compensation was shown to depend upon integration by the gyroscope torque summing member. At that time the effects of any stabilization servo drive associated with the gyroscope when it is used in an inertial system were neglected. A stabilization servo, along with the gyroscope, acts as an integrating drive or space integrator. The integration processes of the gyroscope torque summing member and stabilization servo differ considerably. Their individual contributions to the integration of torques on the torque summing member also differ greatly.

The equation describing integration by the torque summing member, repeated here for convenience, is:

$$\Delta A_{(tsm)} = \frac{1}{C_d} \int_0^t M_{(tsm)}\, dt \qquad (2\text{-}1)$$

In operation $|A_{(tsm)}|$ is limited to a very small value by action of the stabilization servo drive. One function of this drive is to act as an elastic restraint on the gyroscope torque summing member to keep it operating at null. How well this function is performed

determines how large $|A_{(tsm)}|$ may become and therefore how much integration is performed by the viscous shear process in the gyroscope.

A block diagram of the essential components of a single-axis stabilization servo drive appears in Figure 3-1. In an inertial navigation system three of these drives are generally required. While the actual servo instrumentation of a three-axis gimbal system is more complex than merely having three independent single-axis drives, the operation of each individual drive can be looked upon as being similar to Figure 3-1. Besides providing elastic restraint for the gyroscope torque summing member, the stabilization servo drive also produces, under steady-state conditions, an angular velocity about the gyroscope input axis proportional to the torque produced by the torque generator. For an ideal servo drive, this velocity is:

$$\omega_{I(cm)} = \frac{M_{(tg)}}{H} \tag{3-1}$$

where

$\omega_{I(cm)}$ = angular velocity of controlled member (gyroscope and platform on which it is mounted) about gyroscope input axis, relative to inertial space

H = angular momentum of gyro wheel

Hence:

$$\Delta A_{I(cm)} = \frac{1}{H}\int_0^t M_{(tg)}\, dt \tag{3-2}$$

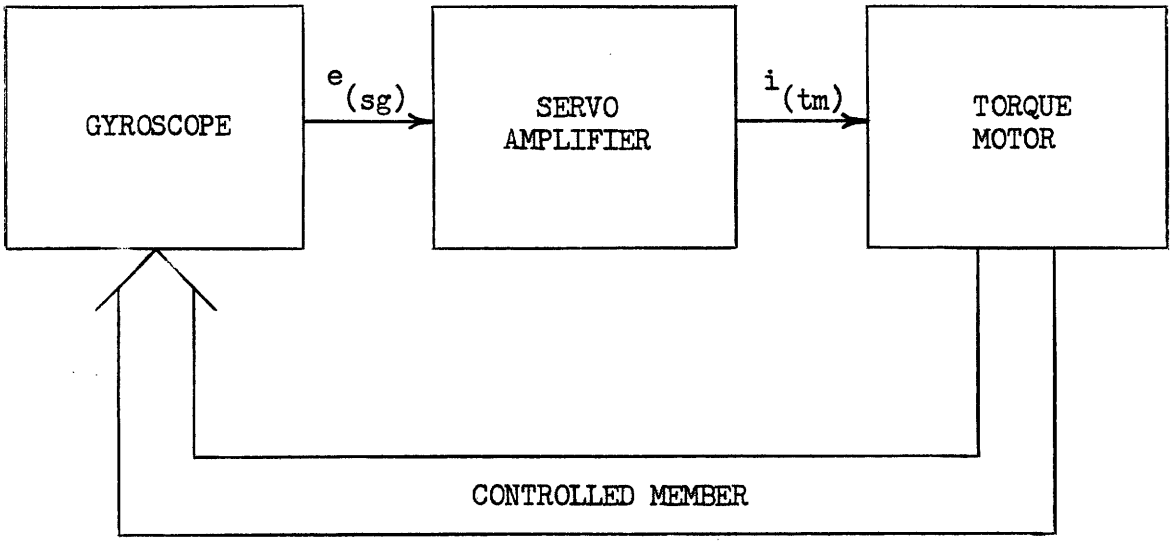

Figure 3-1 Simplified Block Diagram of Single-Axis Gyroscope Stabilization Drive

where

$\Delta A_{I(cm)}$ = rotation of controlled member

For an ideal servo drive with infinite loop gain, no gimbal bearing friction and zero null indication by the gyroscope signal generator, $|A_{(tsm)}|$ is always zero. All of the torque integration is therefore performed by the servo drive. However, for an actual servo drive in which all of the above quantities are finite, the servo drive requires that $|A_{(tsm)}|$ have a certain minimum value, $|A_{(tsm)(min)}|$, before it can respond. This minimum angular deviation corresponds to the gyroscope signal generator output level that produces a servo drive torque that just overcomes the gimbal bearing friction. In actual servo drives, this deviation may be several seconds of arc. During the time that $|A_{(tsm)}|$ is less than $|A_{(tsm)(min)}|$, all torque integration is done by the gyroscope torque summing member.

The controlled member position is generally used as an angular reference in inertial systems. Therefore movements of the gyroscope torque summing member do not effect the angular reference until they are transmitted, via the stabilization servo, to the controlled member. Hence if the digital compensation torque is applied in such a manner that $|A_{(tsm)}|$ is always less than $|A_{(tsm)(min)}|$, ignoring precessional torques, angular deviations of the torque summing member from null, due to the differences between the error torque and compensation torque, will not effect the angular reference. If this type

of operation is assumed, then the effects of the stabilization servo drive on the operation of the digital compensation system can be ignored. The only times that the servo drive will perform angular integrations is when precessional torques or command torques cause the torque summing member to rotate or when rotations caused by compensation torque inaccuracies or uncertainty torques build up to the point that $|A_{(tsm)(min)}|$ is exceeded. In view of this, only torque integration performed by the gyroscope torque summing member will be considered here as to its possible effects on digital compensation.

Non-linearities and imperfections in components can cause deviations in digital compensation performance from the ideal. The more important of these causes are analyzed in this chapter. In some of the analyses, in order to consider certain effects, the torque acting on the torque summing member due to the combination of error and compensation torques must be known. This torque, of course, depends upon many factors and is always changing. Therefore to facilitate the analyses a certain torque pattern occurring during a given time interval is considered as typical. This torque pattern is given here and then referred to as needed.

In general, the compensation torque is constant in amplitude over a given time interval whereas the drift torque is not. Also, the compensation torque magnitude is generally greater than that of the error torque. Figure 3-2 shows a constant compensation torque of magnitude M_C occurring during the time interval $t_o \rightarrow t_1$ and an error torque of

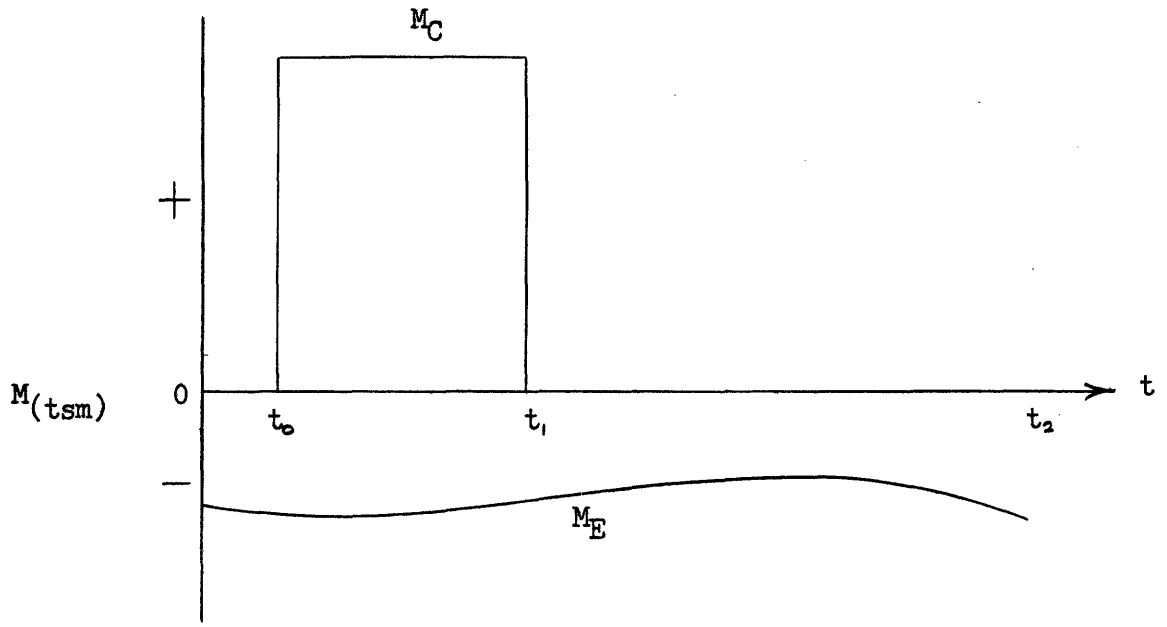

(a)

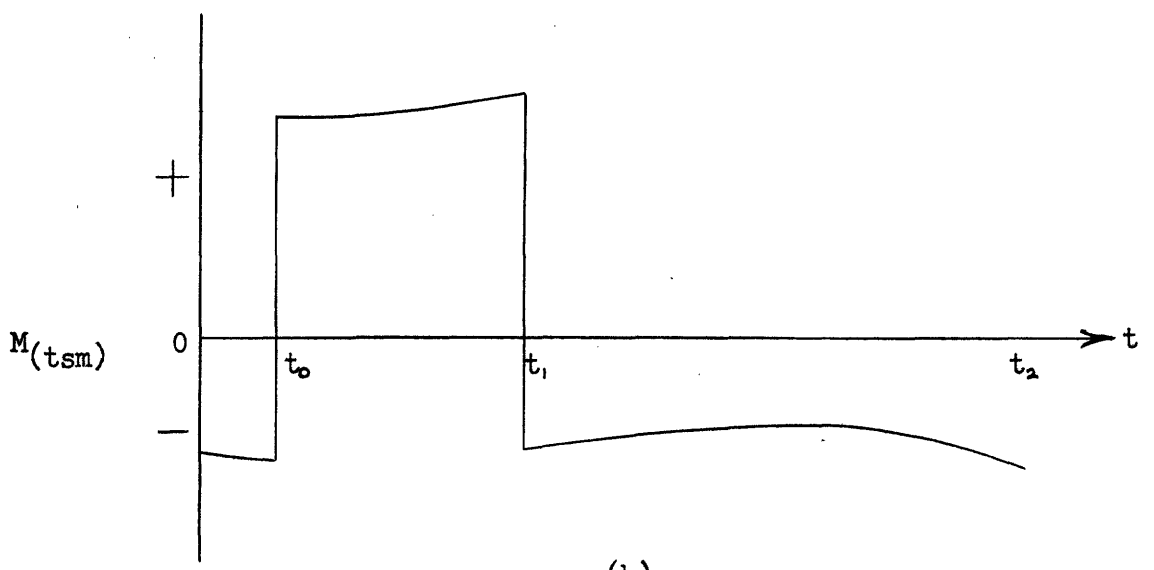

(b)

Figure 3-2 Typical Torque Acting On Torque Summing Member

magnitude M_E, not necessarily constant, occurring continuously. The combined torques produce the net torque acting on the torque summing member shown in part (b). This is the typical torque. The torque has the following properties:

$$|M_C| > |M_E| \text{ (maximum) and } M_C\,(t_1 - t_o) = -\int_{t_o}^{t_2} M_E\, dt \qquad (3\text{-}3)$$

If this torque were applied to a perfect gyroscope, $\Delta A_{(tsm)(t_o \longrightarrow t_2)}$ would equal zero, where $\Delta A_{(tsm)(t_o \longrightarrow t_2)}$ is the angular change of the torque summing member over the interval $t_o \longrightarrow t_2$. Likewise:

$$\Delta A_{(tsm)(t_o \longrightarrow t_1)} = -\Delta A_{(tsm)(t_1 \longrightarrow t_2)} \qquad (3\text{-}4)$$

3.2 Effects of Non-Newtonian Damping Fluid

The damping fluid used in gyroscopes is assumed to exhibit perfect Newtonian qualities. That is, its viscosity is independent of all influences except temperature. It is further assumed that the fluid flow, due to any float movements, is completely laminar. Under these conditions, with constant fluid temperature, the viscous resisting torque exerted on the gyroscope float, as it rotates relative to the case, is given by the equation:

$$M_d = -C_d \frac{dA_{(tsm)}}{dt} \qquad (3\text{-}5)$$

where

M_d = viscous torque exerted on the float by the damping fluid.

Rewritten, this equation becomes:

$$\Delta A_{(tsm)} = \frac{-1}{C_d} \int_0^t M_d \, dt \qquad (3\text{-}6)$$

This relationship is the source of the integrating properties of the gyroscope.

If either or both of the above assumptions concerning the damping fluid is not realized in practice, the integration performed by the gyroscope is affected. In an inertial system not employing digital drift compensation, anomalies in gyroscope integration do not greatly effect system performance, since, as pointed out previously, practically all angular integration is performed by the stabilization servo drives. However, when digital drift compensation is employed, integration performed by the gyroscope float should prove more critical, since such compensation depends heavily on these integrating properties. The number of float movements is greatly increased when digital compensation is used.

In order to determine the effects of a non-Newtonian damping fluid or non-laminar flow on digital drift compensation, a damping torque is considered that is not directly proportional to the relative angular velocity of the float and case. Such a condition would exist for non-laminar flow or for a fluid whose viscosity is a function of shear rate. An arbitrary non-linearity will be assumed such that:

$$M_d = -C_d \left[\frac{dA_{(tsm)}}{dt} \right]^b \qquad (3\text{-}7)$$

where

$$b \neq 1$$

For a constant forcing torque, $M_{(tsm)}$, under steady-state conditions, $M_{(tsm)} = - M_d$. Due to the high damping in gyroscopes the torque summing member time constant is very small and hence steady-state conditions are reached quite fast. Therefore transient effects will be ignored here.

For the typical torque of Figure 3-2:

$$M_C + M_E = C_d \left[\frac{dA_{(tsm)}}{dt}\right]^b \tag{3-8}$$

Solving for $A_{(tsm)}$ yields:

$$A_{(tsm)(t_o \longrightarrow t_2)} = \left[\frac{1}{C_d}\right]^b \int_{t_o}^{t_2} \left| M_C + M_E \right|^{\frac{1}{b}} dt \tag{3-9}$$

If M_E is constant during the interval $(t_o \longrightarrow t_2)$:

$$\Delta A_{(tsm)(t_o \longrightarrow t_2)} = \left[\frac{1}{C_d}\right]^b \left[\left| M_C + M_E \right|^{\frac{1}{b}} (t_1 - t_o) - \left| M_E \right|^{\frac{1}{b}} (t_2 - t_1) \right] \tag{3-10}$$

For the typical torque of Figure 3-2, with M_E constant:

$$\frac{t_1 - t_o}{t_2 - t_1} = \frac{\left| M_E \right|}{\left| M_C + M_E \right|} \tag{3-11}$$

Therefore,

$$\Delta A_{(tsm)(t_o \longrightarrow t_2)} = \frac{\left| M_C \right| (t_2 - t_1)}{(C_d)^b} \left[\left| M_C + M_E \right|^{\frac{1}{b} - 1} - \left| M_E \right|^{\frac{1}{b} - 1} \right] \tag{3-12}$$

Thus, $\Delta A_{(tsm)(t_o \longrightarrow t_2)} = 0$ only for the isolated case when $|M_C| = 2 |M_E|$. For all other cases $\Delta A_{(tsm)(t_o \longrightarrow t_2)}$ has some value which represents the error introduced by imperfect float integration during the interval $t_o \longrightarrow t_2$. This error accumulates as long as the error torque remains in the same direction.

3.3 Effects of Damping Fluid Temperature Changes

The gyroscope damping fluid temperature is usually maintained within certain limits by a system of electric heating coils located around the fluid chamber. Temperature sensing devices control the amount of current flowing to these heating coils. In the gyroscope used for this thesis, a temperature sensitive microswitch, which was either off or on, controlled the current to the heaters.

One formula for the viscosity of a fluid as a function of temperature is given by:

$$\log \mu = \frac{A}{T} + B \qquad (3\text{-}13)$$

where

T = absolute temperature of fluid

A, B = fluid constants

Other formulas exist, all of which relate viscosity exponentially with temperature. Within a narrow temperature range, however, a good approximation is obtained by using a linear relationship between viscosity and temperature.

For the gyroscope used for this thesis, the viscosity of the

damping fluid increases approximately 4% for each drop of 1° F in temperature in the immediate vicinity of the operating temperature. This change can therefore be approximately described by the formula:

$$\mu_o = \mu \ (1 + 0.04 \ [T_o - T]) \qquad (3\text{-}14)$$

where

μ_o = viscosity at specified operating temperature, T_o

μ = viscosity at actual operating temperature, T

The design specifications of this gyroscope called for temperature control limits of ± 0.2° F. The fluid temperature therefore fluctuated between T + 0.2° and T - 0.2°. Under the ambient conditions of normal room temperature, the duty cycle of the microswitch was measured to be approximately 1.8 seconds on and 7.8 seconds off.

If a linear rise and fall in fluid temperature between the operating temperature limits is assumed, then the damping fluid viscosity of the gyroscope under consideration changes with time as shown in Figure 3-3. The maximum change in viscosity over each temperature cycle is 1.6%.

For a given forcing torque acting on the torque summing member, $\frac{dA_{(tsm)}}{dt}$ is proportional to $\frac{1}{C_d}$ and also to $\frac{1}{\mu}$, since C_d is proportional to μ. The float therefore rotates faster when μ is lower. If the majority of the compensation torque pulses occur when μ is higher than μ_o or when μ is lower than μ_o errors in $A_{(tsm)}$ are introduced. These errors are a source of uncertainty. In general the errors cancel

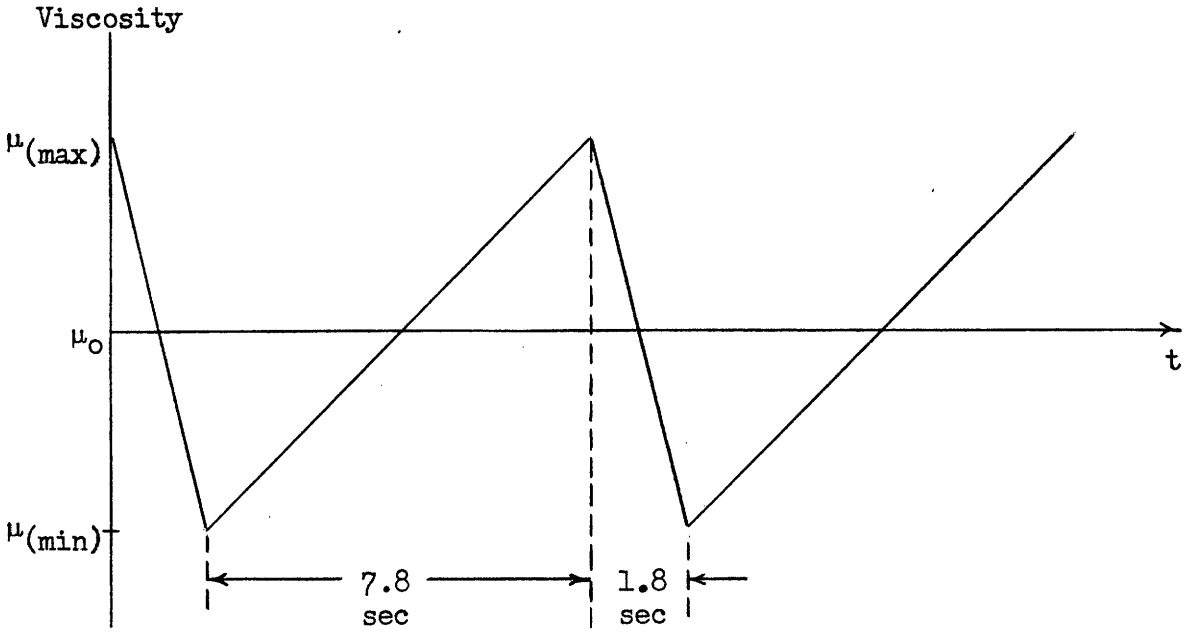

Figure 3-3 Ideal Viscosity Changes of Test Gyroscope Damping Fluid

out over periods of time and therefore do not accumulate. However, if the compensation torque application cycle is some multiple of the fluid temperature cycle, these errors may accumulate. In the worst case, when compensation torque applications occur once each temperature cycle, at the time of maximum or minimum viscosity, the error introduced in $A_{(tsm)}$ each cycle is:

$$(E)A_{(tsm)} = \Delta A_{(tsm)(max)} \frac{\mu_{(max)} - \mu_{(min)}}{2\,\mu_o} \qquad (3\text{-}15)$$

where

$\Delta A_{(tsm)(max)}$ = maximum torque summing member deviation with constant fluid temperature.

The damping fluid temperature is not uniform. Due to the distribution of the heaters, temperature gradients are present throughout the fluid. Therefore viscosity gradients are also present. The presence of convection currents and changes in F make the effects of the viscosity gradients practically impossible to analyze. These gradients are therefore a source of uncertainty torque.

3.4 Effects of Friction in Torque Summing Member Suspension

The pivot and jewel suspension of the gyroscope torque summing member can be the source of undesired non-viscous friction torques. These torques are partially dependent upon the suspension loading, which in turn depends upon the buoyancy of the damping fluid and upon F. The buoyancy of the damping fluid varies with its density, which is a function of temperature. Therefore the suspension friction is not constant,

but varies with F and fluid temperature.

For purposes of this discussion, the suspension friction torque, $M_{(sf)}$, is assumed to have a magnitude $|M_{(sf)(max)}|$ as long as the magnitude of $M_C + M_E$ is equal to or greater than this amount and to be equal in magnitude to $M_C + M_E$ otherwise. The direction of $M_{(sf)}$, of course, is opposite to that of $M_C + M_E$.

For the typical torque of Figure 3-2:

$$\Delta A_{(tsm)(t_o \longrightarrow t_2)} = \frac{1}{C_d}\left[M_C(t_1 - t_o) + \int_{t_o}^{t_2} M_E dt + \int_{t_o}^{t_2} M_{(sf)} dt\right] \tag{3-16}$$

If M_C and M_E are both greater than $M_{(sf)(max)}$ then:

$$\Delta A_{(tsm)(t_o \longrightarrow t_2)} = \frac{1}{C_d}\left[M_C(t_1 - t_o) + \int_{t_o}^{t_2} M_E dt - |M_{(sf)(max)}|(t_1 - t_o) + |M_{(sf)(max)}|(t_2 - t_1)\right] \tag{3-17}$$

By definition the sum of the first two terms of (3-17) equals zero. Therefore:

$$\Delta A_{(tsm)(t_o \longrightarrow t_2)} = \frac{1}{C_d}|M_{(sf)(max)}|\left[(t_2 - t_1) - (t_1 - t_o)\right] \tag{3-18}$$

In general $(t_2 - t_1) \neq (t_1 - t_o)$. The usual case is for $(t_2 - t_1)$ to be several times larger than $(t_1 - t_o)$.

If M_E is smaller than $M_{(sf)(max)}$, then:

$$\Delta A_{(tsm)(t_o \rightarrow t_2)} = \frac{1}{C_d} \left[M_C(t_1 - t_o) + \int_{t_o}^{t_2} M_E dt - \left| M_{(sf)(max)} \right| (t_1 - t_o) - \int_{t_1}^{t_2} M_E dt \right] \tag{3-19}$$

or,

$$\Delta A_{(tsm)(t_o \rightarrow t_2)} = \frac{1}{C_d} \left[(M_C - \left| M_{(sf)(max)} \right|) (t_1 - t_o) + \int_{t_o}^{t_1} M_E dt \right] \tag{3-20}$$

When M_E is smaller than $M_{(sf)(max)}$, M_C will always be much greater than both these torques. Therefore the result in both cases is an error in $\Delta A_{(tsm)}$ in the direction of M_C. This error accumulates as as long as M_E remains in the same direction.

3.5 Effects of $A_{(tsm)}$ Not being Zero

It has been shown[4*] that the mutual inductance of the Microsyn torque generator excitation and input windings is proportional to $A_{(tsm)}$. Thus, for finite excitation and input source impedances and $A_{(tsm)} \neq 0$, cross-coupling currents flow in the two windings. The torque produced by the torque generator then becomes:

$$M_{(tg)} = S_{(tg)} \left[i_{(ex)(tg)(ideal)} \, i_{(in)(tg)(ideal)} + i_{(ex)(tg)(ideal)} \, \delta i_{(ex)(tg)} + i_{(in)(tg)(ideal)} \delta i_{(in)(tg)} + \delta i_{(ex)(tg)} \, \delta i_{(in)(tg)} \right] \tag{3-21}$$

*superscripts refer to Bibliography

where

$$i_{(ex)(tg)} = i_{(ex)(tg)(idea)} + \delta i_{(in)(tg)}$$

$$i_{(in)(tg)} = i_{(in)(tg)(ideal)} + \delta i_{(ex)(tg)}$$

$$\delta i_{(ex)(tg)} = \frac{v_{(ex)(tg)}\ \omega\ (ML)_{(ex)(in)}}{Z_{(equiv)(ex)(tg)} Z_{(equiv)(in)(tg)}} \qquad (3\text{-}22)$$

$$\delta i_{(in)(tg)} = \frac{v_{(in)(tg)}\ \omega\ (ML)_{(ex)(in)}}{Z_{(equiv)(in)(tg)} Z_{(equiv)(ex)(tg)}} \qquad (3\text{-}23)$$

where

$v_{(ex)(tg)}$

and $v_{(in)(tg)}$ = open circuit voltages of the respective torque generator winding power sources

ω = angular frequency of the voltages

$(ML)_{(ex)(in)}$ = mutual inductance of the two windings

$Z_{(equiv)(ex)(tg)}$

and $Z_{(equiv)(in)(tg)}$ = equivalent impedances of the respective torque generator windings. Each is equal to the source impedance plus the winding impedance.

$$i_{(ex)(tg)(ideal)} = \frac{v_{(ex)(tg)}}{Z_{(equiv)(ex)(tg)}} \qquad (3\text{-}24)$$

$$i_{(in)(tg)(ideal)} = \frac{v_{(in)(tg}}{Z_{(equiv)(in)(tg)}} \qquad (3\text{-}25)$$

Since the cross-coupling currents are generally very small compared to the applied currents, the last term of (3-21), which is the product of these two currents, is ignored. The mutual inductance is directly proportional to $A_{(tsm)}$ and ideally zero at $A_{(tsm)} = 0$. It can therefore be written, $(ML)_{(ex)(in)} = K_{(ML)}A_{(tsm)}$, where $K_{(ML)}$ is a proportionality constant. Rewritten, equation (3-21) becomes:

$$M_{(tg)} = S_{(tg)} \left[i_{(ex)(tg)(ideal)} \, i_{(in)(tg)(ideal)} + i^2_{(ex)(tg)(ideal)} \frac{K_{(ML)}A_{(tsm)}}{Z_{(equiv)(in)(tg)}} + i^2_{(in)(tg)(ideal)} \frac{K_{(ML)}A_{(tsm)}}{Z_{(equiv)(in)(tg)}} \right] \qquad (3\text{-}26)$$

The last two terms on the right of (3-26) are directly proportional to $A_{(tsm)}$. They represent a torque that aids the ideal torque of the first term when $A_{(tsm)}$ is on one side of null and opposes the ideal torque when $A_{(tsm)}$ is on the other side of null. Thus these two terms cause an elastic torque to be added to the ideal torque. For torque generator winding impedances usually encountered, this torque is stable. Such a torque is undesirable for the proper operation of the gyroscope, since it is a non-integrating elastic restraint acting on the torque summing member.

When precession torques cause the torque summing member to rotate

from null, this elastic torque tends to force the torque summing member back to null. This introduces an error equal to the angle through which the torque summing member moves toward null due to action of the elastic torque. The error is opposite in direction to the precession torque. Therefore as long as the precession torques remain in the same direction the individual errors will accumulate.

In order to reduce the effects of cross-coupling currents the equivalent impedances should be as high as possible. This requires using sources with high output impedances.

Due to increasing mutual inductance with increasing $\left|A_{(tsm)}\right|$ an elastic torque is also produced by the signal generator Microsyn when a finite load is placed on the secondary winding. For a resistive or inductive load the elastic torque is stable. However, for a capacitive load the torque becomes unstable. An unstable torque causes any deviations of the torque summing member from null to increase with time. Any unstable elastic torque produced by the signal generator is generally smaller in magnitude than the stable elastic torques produced by the torque generator and electrical leads. Therefore the net elastic torque on the torque summing member is stable.

3.6 Effects of Switching Errors and Transients

Equations (2-1) and (1-2) combine to give the torque summing member rotation due to torque generator currents as:

$$\Delta A_{(tsm)} = \frac{S_{(tg)}}{C_d} \int_0^t i_{(ex)(tg)} i_{(in)(tg)} dt \qquad (3\text{-}27)$$

Therefore $\Delta A_{(tsm)}$ depends upon the waveshape of the input current as well as its application time. Until now the input current has been assumed to be either sinusoidal or constant during the time it is applied. In practice, however, transients may alter the waveshape of the input current and therefore cause $\Delta A_{(tsm)}$ to be different than desired. Also timing errors in the application of the input current can effect $\Delta A_{(tsm)}$. Since the excitation current is applied continuously, transients and timing errors are not factors in its contribution to the torque.

In the torque control methods described in Chapter II, the torque generator input current is controlled by electronic switches. Since the torque generator windings are highly inductive, if direct current is used a transient build-up of current to the desired level occurs when the switch is turned on. A transient also occurs when the switch is turned off.

A square voltage pulse applied to the torque generator input winding causes a current pulse similar to that of Figure 3-4a. Since the winding behaves as a series RL circuit the rise and fall transients of this current pulse are equal, i. e., area A equals area B. Hence the area of such a pulse is the same as one with no transient effects. The excitation current is constant and so $\Delta A_{(tsm)}$ is proportional to the input current pulse area. Therefore symmetrical transients do not affect $\Delta A_{(tsm)}$. The transients do shift the centroid of the pulse area in time, which makes the compensation take place slightly later

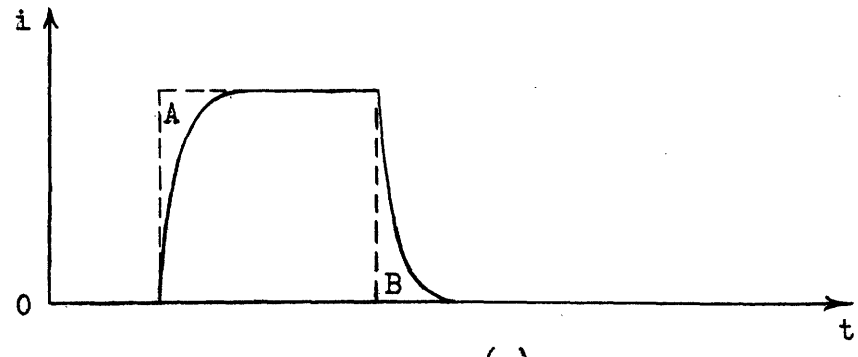

(a)

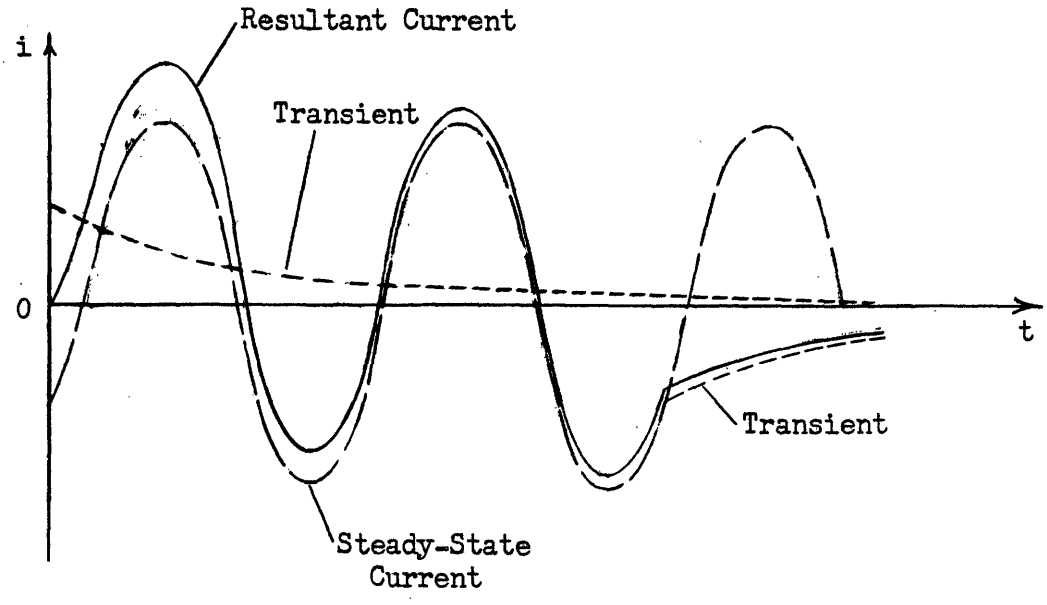

(b)

Figure 3-4 Torque Generator Input Current Waveforms Showing Transients Caused By Switching

than planned. This effect, however, is not too significant.

Factors other than simple exponential build-up and decay affect the current pulses, however. The transient characteristics of the electronic switch and its associated flip flop also determine the pulse shape. The circuits that were used for this thesis employed semiconductors. For these circuits, the fall times of torque generator input current pulses were greater than the rise times. This result was due in part to minority carrier storage in the transistors. Such circuit non-linearities cause the voltage pulse to be not perfectly square.

For actual switching circuits, then, the rise and fall transients are generally not symmetrical. The area of such a pulse is not the same as one without transients. Therefore the area is not directly proportional to the presumed application time of the voltage pulse. Since in the torque control methods discussed, time is the controlled variable, using equally spaced clock pulses, errors result if the voltage pulse duration is different than that at which the torque is originally calibrated.

Besides transients, timing errors affect the area of the current pulses. If time delays occur between a turn-on command pulse and the operation of the switch, the current pulse does not start until later than desired. Similarly turn-off delays in the switch cause the current pulse to end later than desired. For direct current pulses, the area is not affected if both these delays are equal. If, however, they are

unequal, the area is either smaller or greater than desired, depending upon the size of each delay.

When alternating current is used on the torque generator windings transients can be effectively eliminated by switching the input current when the steady-state current sine wave pases through zero. This makes the timing of the switch operation critical. Any deviation of the switching times will cause transients. The equation of the current resulting from the sudden application of a sinusoidal voltage to a series RL circuit at t = 0 is:

$$i = \frac{E}{Z} \sin(\omega t + \lambda - \theta) - \frac{E}{Z} \sin(\lambda - \theta)\, e^{-(R/L)t} \qquad (3\text{-}28)$$

where

θ = steady-state phase angle between voltage and current

λ = phase angle of voltage when voltage is applied

If the voltage is then removed at time t_1 the current becomes:

$$i = \frac{E}{Z} \sin(\omega t_1 + \lambda - \theta) e^{-(R/L)(t - t_1)} - \frac{E}{Z} \sin(\lambda - \theta) e^{-(R/L)t} \qquad (3\text{-}29)$$

The transient terms are zero if $\lambda = \theta$. Figure 3-4b shows the approximate shape of such a current wave for two cycles of applied voltage, using arbitrary λ and θ. The resultant waveform consists of the sum of the two transients and the steady-state term. Any errors in $\Delta A_{(tsm)}$ result only from the transient terms.

If the torque generator excitation current is in phase with the steady-state input current, the error in $\Delta A_{(tsm)}$ caused by transients

is:

$$(E)\Delta A_{(tsm)} = \frac{S_{(tg)}I_{(ex)(tg)}I_{(in)(tg)}}{2C_d}\left[\int_0^{\infty}\sin(\omega t+\lambda-\theta)\left[-\sin(\lambda-\theta)e^{-(R/L)t}\right.\right. dt$$

$$\left.\left. + \int_{t_1}^{\infty}\sin(\omega t+\lambda-\theta)\left[\sin(\lambda-\theta)e^{-(R/L)(t-t_1)}\right]dt\right]\right. \qquad (3\text{-}30)$$

$$(E)\Delta A_{(tsm)} = \frac{S_{(tg)}I_{(ex)(tg)}I_{(in)(tg)}}{2C_d}\,\frac{\omega}{(R/L)^2+\omega^2}$$

$$\cdot\left[\sin(\omega t_1+\lambda-\theta)-\sin(\lambda-\theta)\right] \qquad (3\text{-}31)$$

If ωt_1 is an integer multiple of 2π, the error is zero. Therefore when a whole number of complete cycles of input current is used the transient effects cancel out.

If a timing error, (E)t exists, so that ωt_1 is not an integer multiple of 2π, then:

$$(E)\Delta A_{(tsm)} = \frac{S_{(tg)}I_{(ex)(tg)}I_{(in)(tg)}}{2C_d}\,\frac{\omega}{(R/L)^2+\omega^2}\,\sin\omega(E)t \qquad (3\text{-}32)$$

Since $\omega(E)t$ is generally a small angle, any error in timing causes a proportionate error in rotation of the torque summing member. Timing error effects are more or less independent of the frequency of the currents used, for while the sine term increases with frequency the other factor decreases.

The above discussion of alternating current timing effects assumes the use of linear devices. The transient characteristics of the switching devices used affect the current transients. Therefore even if complete cycles of input current are used, any transients generally

do not cancel. However, any transients resulting from alternating current switching errors usually are much smaller than transients resulting from the use of direct current for the torque generator.

3.7 Quantization Errors

Neglecting the error producing sources discussed previously, digital compensation still produces instaneous errors in float position. These errors are caused by the net torque on the torque summing member due to the compensation torque not being equal and opposite to the error torque at all times. The net torque is caused by compensation torque computation time lags and quantization errors due to the digital approximation of the error torque.

As mentioned previously, a digital compensation system should insure that any instantaneous float position errors caused by quantization should be less than $\left|A_{(tsm)(min)}\right|$. In this way the errors do not appear at the angular reference through operation of the stabilization drive when no precession torque is present. If the compensation torque is applied at equal intervals, then the maximum time between torque applications is:

$$\Delta t_{M(max)} = \frac{C_d}{M_{C(max)}} \Delta A_{(tsm)(min)} \qquad (3\text{-}33)$$

where

$M_{C(max)}$ = maximum compensation torque

$\Delta A_{(tsm)(min)} = 2\left|A_{(tsm)(min)}\right|$

If a precession torque acts on the torque summing member so that $|A_{(tsm)(min)}|$ is exceeded, the maximum instaneous error introduced to the angular reference by compensation torque quantization is $\Delta A_{(tsm)(min)}$. Any value less than $\Delta t_{M(max)}$ can be given to Δt_M with a proportionate reduction in the maximum quantization error.

3.8 Computation Errors

Digital computations of the error torque must be made periodically in order to determine the compensation torque required. The time between computations must be equal to or less than Δt_M. Besides this restriction, other factors, which will be discussed, determine the computation interval, Δt_c.

In making the computations, specific force measurements are required from the system accelerometers. In general digital accelerometers produce output pulses proportional to velocity in either of the two directions along their input axes. The equation for the velocity output is:

$$v = S_v (n_{(+)} - n_{(-)}) = S_v n \qquad (3\text{-}34)$$

where

v = velocity along positive direction of accelerometer input axis

S_v = velocity increment per output pulse

$n(+)$ and $n(-)$ = number of output pulses for the positive and negative input axis directions

Acceleration is obtained from this information by differentiating:

$$a = \frac{S_v \Delta n}{\Delta t_c} \tag{3-35}$$

The net number of output pulses, Δn, must be an integer. Therefore it can be in error by as much as one pulse. Since the absolute error in Δn is constant, the relative error can be reduced by increasing Δn. This can only be done by increasing Δt_c, since $\frac{\Delta n}{\Delta t_c}$ is determined by the specific force.

Once an unbalance torque computation has been made, this computation is the only information the system has available concerning the error torque until the next computation. Therefore if the error torque changes during this interval, due to changes in specific force, the available information is in error. This quantization error can be reduced by reducing Δt_c.

Thus two conflicting requirements for Δt_c exist. The compromise that is made in Δt_c between the above two requirements is dictated by individual inertial system operating conditions. If it is known that a system will encounter relatively long periods of constant specific force with infrequent changes that last only for short intervals, Δt_c should be large. However, a system that encounters frequent specific force changes might require a smaller Δt_c. The effects of Δt_c on the computed error torque are now analyzed.

In order to simplify the analysis of the effects of Δt_c on the

error torque computations, equation (1-6) is modified. Essentially (1-6) contains three types of terms: a constant term, terms dependent directly on specific force components and terms dependent on the products of two specific force components. The equation can therefore be written, for a force in any one direction, as:

$$M_E = K_1 + K_2F + K_3F^2 \tag{3-36}$$

where

F = magnitude of mass reaction force on gyroscope

K_2 and K_3 = factors dependent upon direction of F

The equation, written with uncertainties in F, is:

$$M_E = K_1 + K_2\left[F + U(F)\right] + K_3\left[F + U(F)\right]^2 \tag{3-37}$$

Assuming that the uncertainty in F is due to the uncertainty in Δn, i. e., any uncertainty in Δt_c is small compared to the uncertainty in Δn, then:

$$F + U(F) = \frac{(\Delta n+1)S_v}{\Delta t_c} \tag{3-38}$$

When this substitution is made, (3-37) becomes:

$$M_E = K_1 + K_2F + K_3F^2 + \frac{S_v}{\Delta t_c}\left(K_2 + 2K_3\frac{\Delta n+1}{\Delta t_c}\right) + K_3\left(\frac{S_v}{\Delta t_c}\right)^2 \tag{3-39}$$

The relative uncertainty in M_E is:

$$\frac{\left(\frac{1}{\Delta t_c}\right)^2\left[2K_3S_v(\Delta n+1) + K_3S_v^2\right] + \frac{1}{\Delta t_c}(K_2S_v)}{M_E} \tag{3-40}$$

The relative uncertainty in M_E increases as Δt_c is decreased. This un-

certainty holds for each unbalance torque computation and the actual error may be positive or negative. For constant F, generally one computation will be in error on the high side and the next computation in error on the low side, since a velocity pulse which is omitted by one sampling interval is gained by the next one. However, since M_E is not a linear function of F, equal positive and negative errors in two separate computations of M_E do not produce cancelling effects. Therefore when these individual computations are summed up, either digitally or by the integrating action of the gyroscope, the compensation torque-time integral will be larger than required.

The effects of Δt_c on the quantization error in F cannot be determined, since the actual variations of F with respect to time must be known. However, the effects for an assumed linear variation of F with respect to time can be found by considering Figure 3-5a. This figure shows a linear increase and decrease in F, each of equal amounts and occurring over equal time intervals. Here $\frac{dF}{dt}$ is constant and $\Delta F = \frac{dF}{dt} \Delta t_c$, where ΔF is the quantization error in F. The effect of ΔF on M_E computations can be found by substituting ΔF for U(F) in (3-37). This gives:

$$M_E(\text{computed}) = K_1 + K_2F + K_3F^2\ \Delta F(K_2 + 2K_3F) + K_3(\Delta F)^2 \qquad (3\text{-}41)$$

Figure 3-5b shows the changes in M_E corresponding to the changes of F in part (a). The effect of Δt_c on the error torque quantization error, ΔM_E, can be seen from the following:

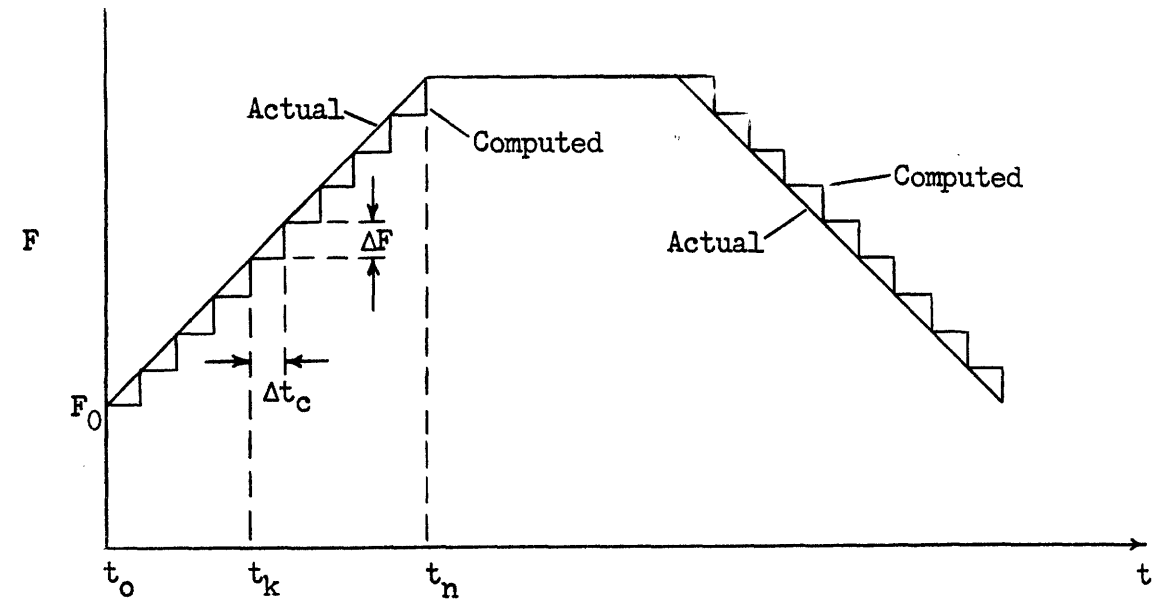

(a)

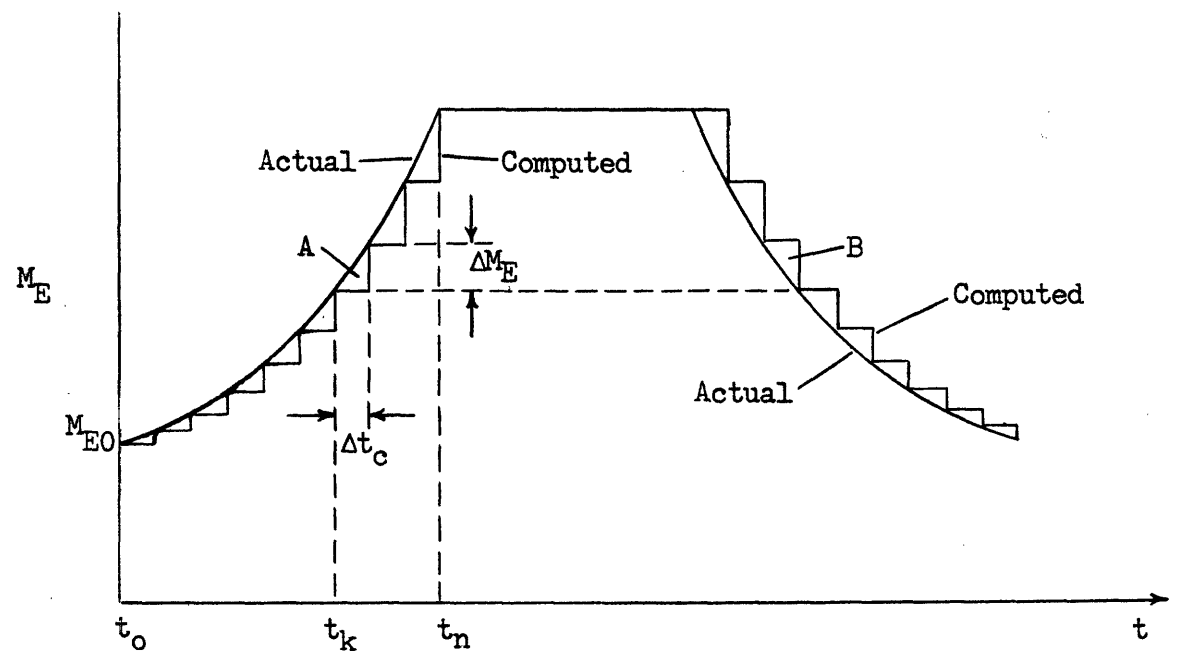

(b)

Figure 3-5 Computed Error Torque Quantization

$$\Delta M_E = \Delta t_c(K_2K_F + 2K_3FK_F) + \Delta t_c{}^2(K_F)^2K_3 \qquad (3\text{-}42)$$

where

$$K_F = \frac{dF}{dt}$$

ΔM_E, beside being a function of Δt_c, also depends on F and increases with increasing F.

The important consideration of the error torque quantization is that the computed quantity, $\int M_E dt$, should equal the actual quantity, when integrated over a relatively long period of time. Thus, even though instaneous errors are present there should be no cumulative error. A look at Figure 3-5b shows that, between t_o and t_n, $\int M_E dt$(computed) is smaller than $\int M_E dt$ (actual). The amount of the difference is:

$$(E)\int_{t_o}^{t_n} M_E dt(\text{computed}) = \int_{t_o}^{t_n} M_E dt - \sum_{k=0}^{n-1} M_{Ek}\Delta t_c \qquad (3\text{-}43)$$

$$= \int_{t_o}^{t_n} (K_1 + \left[K_2 K_F(t - t_o) + F_o\right] + K_3\left[K_F(t - t_o) + F_o\right]^2)dt$$

$$- K_1(t_n - t_o) + \sum_{k=0}^{n-1}\left[K_2(kK_F\Delta t_c + F_o)\Delta t_c + K_3(kK_F\Delta t_c + F_o)^2\Delta t_c{}^2\right] \qquad (3\text{-}44)$$

where

M_{Ek} = computed error torque at time t_k

Therefore for changing specific force, an error in computing $\int M_E dt$ is introduced which increases with time as long as the force is changing. Once the force is constant again the error remains constant. If this constant error is cancelled when the specific force returns to its original value, no cumulative error is introduced. This possibility is now investigated.

In figure 3-5b, area A and area B are the quantization errors in $\int M_E dt$ for an equal increase and decrease in M_E occurring during Δt_c. Area B is larger than A. It is larger by the amount:

$$B-A = 2\left(\left[M_{Ek} + \frac{1}{2}\Delta M_E\right]\Delta t_c - \int_{t_k}^{t_k+\Delta t_c} M_E dt\right) \tag{3-45}$$

$$B-A = \left[2(K_2F_k + K_3F_k^2) + \Delta t_c\,(K_2K_F + 2K_3K_FF_k + K_3K_F^2\Delta t_c)\right]\Delta t_c$$

$$-2\int_{t_k}^{t_k+\Delta t_c} (K_2\left[K_F(t - t_o) + F_o\right] + K_3\left[K_F(t - t_o) + F_o\right]^2)dt \tag{3-46}$$

$$B-A = \frac{7}{3}K_3K_F^2\Delta t_c^3 \tag{3-47}$$

The net error in $\int M_E dt$, caused by the increase in the magnitude of F and subsequent decrease back to its original value, is: $(t_n - t_o)(\frac{7}{3}K_3K_F^2\Delta t_c^2)$. These errors accumulate as long as F remains in the same direction relative to the gyroscope.

3.9 Other Factors Affecting Digital Compensation

When direct current is used for the operation of the torque generator, hysteresis effects in the torque generator core material cause a residual flux to remain in the core when the input current has ceased. This residual flux depends partly on the input current magnitude and direction at the time it is turned off. The residual flux is in addition to the flux due to the excitation current. Residual flux gives rise to unwanted torques and thus is a source of errors. These errors accumulate as long as the input current is applied in the same direction. In general, hysteresis errors cannot be accurately predicted.

When alternating current is used for operation of the torque generator, the mmf due to the excitation current is alternating and therefore constantly recycling the hysteresis loop. Residual flux is then no longer a problem. A residual flux problem does occur with alternating current, however, when an input current is suddenly applied whose mmf is approximately equal to the excitation mmf. Under these conditions the net mmf at two of the torque generator poles is very low. Any residual flux may then be large compared to the alternating component. This problem can be eliminated by keeping the input and excitation mmf's sufficiently different in amplitude.

The stability of the source supplying torque generator current is important because of its effect on the torque produced by the torque generator. If the same source supplies both input and excitation currents, a small fluctuation in the source voltage causes a percentage fluctuation in torque approximately twice as great, since the torque is proportional to the product of the currents.

Torque generator input current-torque non-linearities caused by non-linearities of the core material do not effect torque control methods 2, 3 and 4, since the compensation torque magnitude is constant for these methods. It is only necessary to initially calibrate the torque at the level used. Method 1 is effected by torque generator non-linearities, since torque level changes occur. These effects can also be overcome, however, by adjusting each individual torque level.

Chapter IV

DIGITAL COMPENSATION TESTS

4.1 Introduction

In order to determine the actual errors present in a digital compensation system, a test setup was constructed. A series 10.0 FG-1-2 floated gyroscope was used for the tests. The gyroscope was mounted on a Griswold rotary table with its output axis coincident with the table axis and perpendicular to the local gravity vector. The gyroscope could thus be rotated about its output axis and its angular position accurately determined by a magnified vernier dial on the rotary table. Oriented in this way, compliances and the mass unbalance about the gyroscope output axis cause a torque to act on the torque summing member due to gravity. Since the position of the gyroscope relative to gravity could be changed by rotating the table, the magnitude and direction of the error torque could be varied. No stabilization servo was used with the gyroscope for reasons stated before. Since the servo was omitted, the gyro wheel did not have to be running. This in turn eliminated the need to cancel out any precession of the gyro wheel due to earth rate.

A block diagram of the test setup used appears in Figure 4-1. This setup was modified for different tests. The intention was not to

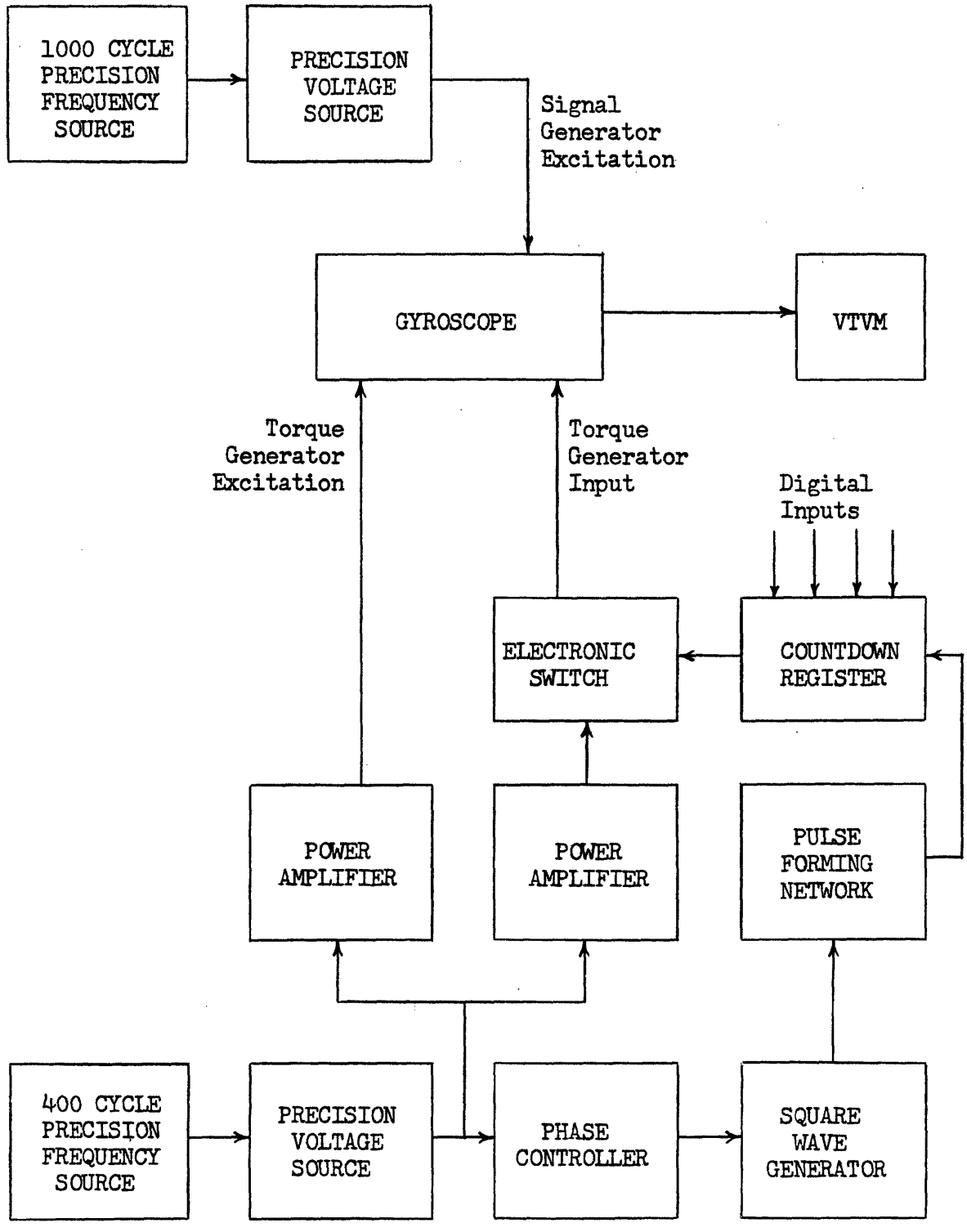

Figure 4-1 Block Diagram of Test Setup

test a complete digital compensation system, since such a test would have necessitated having practically a complete inertial system. A countdown register was used, into which simulated digital computer outputs were fed. Clock pulses were obtained from a square wave derived from the 400 cycle torque generator current. These clock pulses were also used for timing when direct current was used for the torque generator. Both the frequency and amplitude of the torque generator and signal generator currents were precisely controlled. Torque summing member angular position was determined by a V. T. V. M. which monitored the gyroscope signal generator output voltage.

Designing an adequate electronic switch for the tests proved somewhat difficult. The difficulty encountered is that since a transistor is a three terminal device, no possibility exists of isolating the circuit that controls the transistor from the circuit the transistor controls. The electronic switch uses direct current signals to switch alternating current. Relays possess the four terminal operation needed, but are limited by their slow switching characteristics. At first a circuit using four switching transistors in a demodulator-type circuit was tried. Problems were encountered with the alternating current shorting through one-half of the switch on alternate half cycles. This was caused by collector-base conduction in the switching transistors. The circuit finally used is shown in Figure 4-2. Only two transistors are used for the actual switching. When either of the switching transistors is cut off,

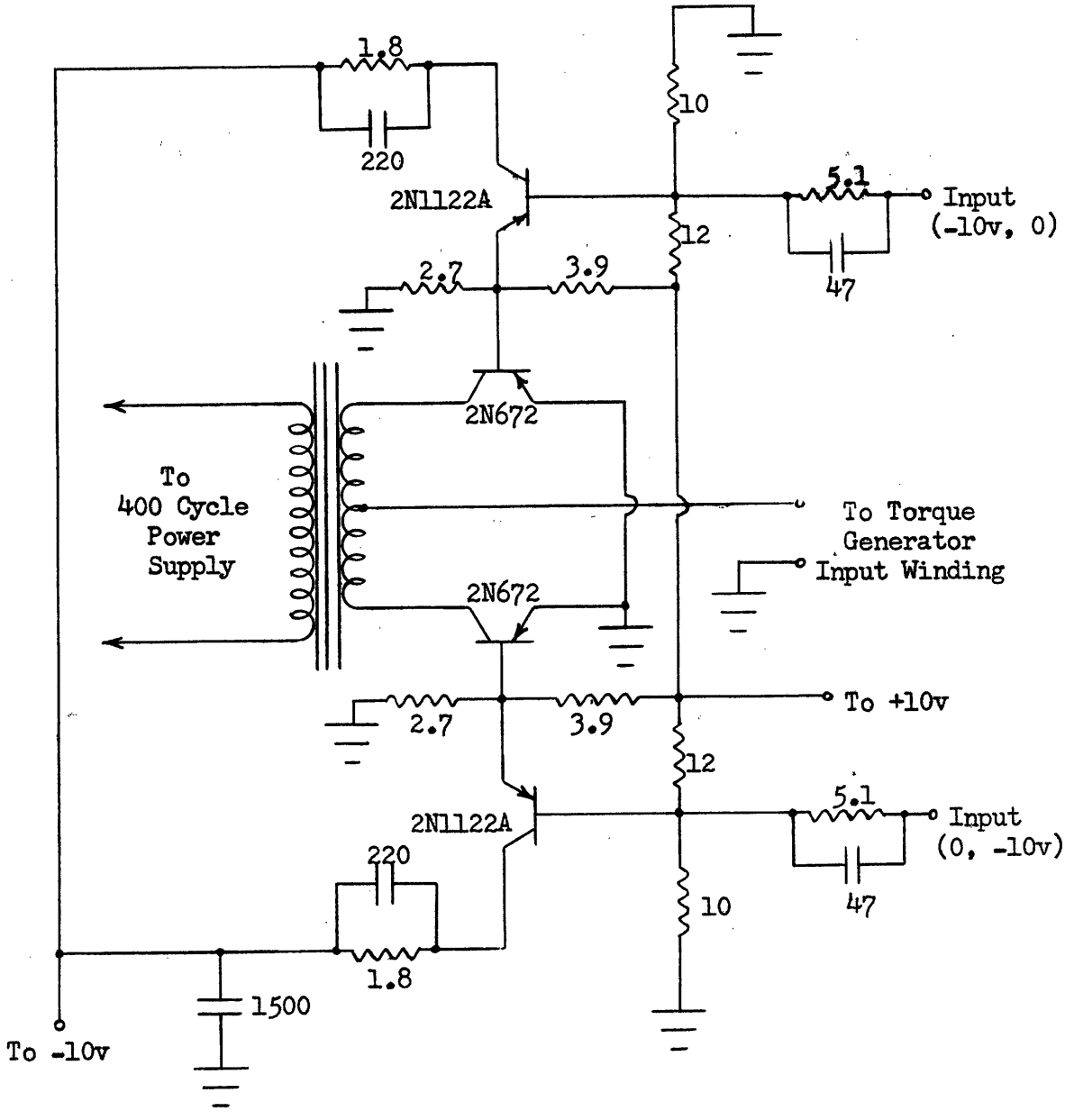

Resistors in kΩ

Condensers in μμf

Figure 4-2 Schematic Diagram of Electronic Switch

its base is biased at a voltage higher than the peak alternating current voltage that appears at the collector. Therefore collector-base conduction is prevented.

The test setup outlined above was first used to determine to what extent certain of the errors discussed in Chapter III affected an actual system. Then, tests were run to see how well the torque control methods described in Chapter II performed.

4.2 Test Methods

A plot of gyroscope unbalance torque as a function of rotary table angular position was first obtained. The torque, for one degree increments of table position, was determined by measuring the torque generator currents required to hold the torque summing member at null for a certain period of time and using available data on torque generator sensitivity. Using this plot, a table angular position could be chosen to obtain a certain unbalance torque about the gyroscope output axis. Likewise an effective torque generator torque could be measured by setting the table at a position that resulted in zero drift of the torque summing member. The curve obtained was correct only when the torque summing member was at null. However, by restricting movements of the torque summing member to approximately 0.1 milliradian either side of null, essentially constant torques were obtained while allowing movements of the torque summing member for purposes of viscous shear integration.

In the following discussion the unit of torque used is meru. Meru,

or milli-earth-rate-unit, is not a torque unit, but an angular rate unit. However, for any given gyro wheel angular momentum, a constant angular rate input to a gyroscope will produce a certain torque about the output axis. A 1 meru torque, therefore, is a torque equal to that produced by a 1 meru input to the gyroscope under consideration.

The drift rate measurements taken during the tests described here were obtained as follows. The reading of the V. T. V. M. monitoring the gyroscope signal generator output was related to the torque summing member position by the signal generator sensitivity. The amount of time for drift of the torque summing member to cause a certain change in meter reading was measured by a manually operated electric timer. A large magnifying glass was used to help determine the meter indications. The drift measurements thus obtained were average rates over the times of observation. The accuracy of the drift measurements was probably determined by the accuracy of the V. T. V. M. and the accuracy of relative drift measurements by the repeatability of the instrument.

4.3 Tests and Results

Test 1 - Effects of Non-Newtonian Damping Fluid, Non-Laminar Flow and Suspension Friction

The following tests were performed to determine any effects caused by non-Newtonian characteristics or non-laminar flow of the gyroscope damping fluid. The tests consisted of setting the position of the rotary table to obtain, for separate tests, three different unbalance

torque magnitudes. Then, once a second, a compensation torque, with a magnitude N times greater than that of the unbalance torque, was applied in the opposite direction for 1/N second.

For each of the three unbalance torques three different compensation torques were applied. The drift rate and direction for each combination of unbalance and compensation torques were measured and are tabulated below. The rates listed are averages of three separate observations each. Each observation was between 10 and 30 minutes in length, depending upon the drift rate.

Under ideal conditions, there should be no drift of the torque summing member from null when the above torques are applied, except for the once per second deviations. Since the torque in one direction is much greater than in the other, producing greater angular velocities of the float in one direction, in the absence of other errors any non-linearity between float angular velocity and damping torque will cause the torque summing member to drift from null. The rate and direction of this drift are dependent upon the damping fluid.

By applying an unbalance torque and using short compensation torque pulses to keep the gyroscope at null, any friction torque present operates against the unbalance torque for a much greater time than against the compensation torque. This causes a drift in the direction of the compensation torque. The separation of the effects of suspension friction from the other effects lies in the interpretation of the results.

TEST 1 RESULTS

Compensation Torque Pulse Magnitude (meru)

Unbalance Torque Magnitude	40	100	400
2	0.1C	0.1C	0.2C
5	0	0.1C	0.3C
20	0.1U	0.2C	0.2C

Drift Rates (meru)

C = direction of compensation torque

U = direction of unbalance torque

Test 2 - Effects of Damping Fluid Temperature Changes

In order to determine what effects the damping fluid temperature limit cycle might have on compensation torque pulses that occurred at extremely unfavorable times, the following test was performed. The coil of a current relay was inserted in the line carrying current to the gyroscope fluid heaters. A battery and pulse forming circuit were connected to the relay contacts in such a way that a pulse could be obtained, either at the instant the relay closed or the instant it opened. The gyroscope was oriented to obtain a certain unbalance torque. A compensation torque pulse to keep the gyroscope at null was then applied in the opposite direction once per temperature limit cycle, being triggered by one of the two pulses available from the relay circuit. Since the compensation torque pulse width was relatively short compared with the periods of time the heaters were either on or off,

the compensation torque could be applied when the fluid temperature was near either its upper or lower limits, depending upon which relay pulses were used to trigger the torque pulses. Damping fluid viscosity changes with temperature caused the gyroscope to drift from null, the rate and direction depending upon the average fluid temperature at the times the compensation torque was applied. These rates were measured.

The period of the temperature limit cycle is not constant, even under ideal steady-state temperature conditions. Therefore the torque summing member drift was due in part to the fact that the time interval between compensation torque pulses was not constant. In order that drift due to this cause could be determined, the number of temperature cycles which occurred during the observation periods were visually counted. As mentioned previously, the period of each temperature cycle was roughly 10 seconds. The ratio of the compensation torque and unbalance torque magnitudes determined the number of temperature cycles that should have occurred during the observation periods. This ratio must equal the ratio of the observation period length to the total time the compensation torque is applied. Any differences were transformed to average drift rates over the observation periods and subtracted from the observed rates. The measured drift rates, corrected for differences in temperature cycle lengths, are listed below. They are the averages of several observations.

TEST 2 RESULTS

Unbalance Torque Magnitude	Pulse Width (sec.)	Fluid Temperature	Drift Rates
20	0.25	high	0.3C
20	0.25	low	0.2U
50	0.50	high	0.7C
50	0.50	low	0.6U

Test 3 - Switching Transient Effects

The effects of torque generator input current transients due to switching were next determined. As before, compensation torque pulses were used to cancel the effects of an unbalance torque on the torque summing member. When alternating current was used on the torque generator windings, the pulses used were one cycle in width and the timing of the clock pulses controlling the switching was varied in order to vary the phase angle of the current when it was switched. In this way, the effects of transients caused by switching not taking place at the proper phase angle could be determined by measuring any gyroscope drifting produced.

When direct current was used on the torque generator windings, the effects of transients were determined by varying the length of the compensation torque pulses used. If the unbalance torque magnitude is varied in direct proportion to the compensation torque pulse length,

no drift should result. Adverse transient effects were determined by measuring any drift produced. The unbalance torque used for the tests was 50 meru.

TEST 3 RESULTS

Steady-State Alternating Current
Phase Angle at Time of Switching

	0°	5°	15°	30°	60°	90°	120°	150°	165°	175°	180°
Drift Rates	0	0.2C	0.6C	1.1C	1.8C	1.9C	0.9C	0.3U	0.4U	0.1U	0

Direct Current Pulse Width (sec.)

	0.0025	0.005	0.0125	0.025	0.05
Drift Rates	3.4C	1.9C	0.8C	0.4C	0.2C

Test 4 - Effects of Torque Generator Core Hysteresis

The effect of residual magnetism due to hysteresis of the torque generator core material was determined by applying direct current to the excitation winding and direct current pulses to the input winding and determining the unbalance torque required to hold the gyroscope at null after the pulses were removed. The core was demagnetized as much as possible before each test by removing both the input and excitation currents and applying a decreasing alternating current to the excitation winding. The residual torques caused by the hysteresis effects of the core material are listed on the following page.

TEST 4 RESULTS

Compensation Torque Pulse Magnitude	Drift Rates	
	Pos. Pulses	Neg. Pulses
50	0.7C	0.8C
200	1.9C	2.1C
800	2.8C	3.3C

Test 5 - Tests of Torque Control Methods

Tests were run to determine how well the torque control methods discussed in Chapter II performed. These tests were limited to the equipment that follows the computer. The tests attempted to determine if the control methods produce effective torques that are proportional to the numerical magnitude of the computer outputs and how constant the effective torques are compared with continuously applied torques.

Torque control method 1, which switches one of several different continuously applied torque levels, could not be tested since the comparisons were based on continuously applied torques. Method 4 is similar in operation to method 3, except that the torque pulse width is constant. Therefore only methods 2 and 3 were tested.

The tests consisted of applying simulated computer outputs to the equipment to compensate for several different magnitudes of gyroscope error torque. Any resulting drift rates were measured. Only results are shown for the tests in which alternating current was used for operation of the torque generator. Such poor results were obtained when

direct current was used that the tests were not continued.

TEST 5 RESULTS

Unbalance Torque Magnitude	Drift Rates	
	Method 2	Method 3
0	0.1U	0
5	0	0.1C
10	0.2C	0.2C
15	0	0.1C
20	0.2C	0.2C
25	0.1C	0.2C
30	0.1U	0
35	0.2U	0
40	0.3U	0.1U
45	0.1U	0.2C
50	0.2U	0.2C

Chapter V

CONCLUSIONS

5.1 Discussion of Test Results

Test 1 - The results of Test 1 are inconclusive to some extent. While most of the measurements seem to indicate the presence of friction torques, some of the individual measurements taken were completely opposite of what they should have been under such circumstances. The results seem to indicate a friction torque equivalent to between 0.1 and 0.2 meru. For the gyroscope used this would correspond to roughly 0.1 dyne-cm.

Effects of non-Newtonian damping fluid or non-laminar flow, which would probably be indicated by drifts in the direction of the unbalance torque, i. e., b greater than 1, did not seem to be present. Even the greatest float angular velocities encountered were probably much less than would be needed to reach non-laminar flow conditions. Also, the damping fluid is very carefully chosen to exhibit pure Newtonian qualities. Therefore any effects due to these causes were probably either in the same range or below the accuracy of the equipment and methods used for the tests.

Test 2 - The results of Test 2 were approximately as anticipated. The compensation torque pulses applied when the damping fluid temperature was near its upper limit caused the torque summing member to drift in the direction of the compensation torque. When the pulses were applied while the damping fluid temperature was near its lower limit a drift was caused

in the direction of the unbalance torque. The drift rates were somewhat larger than would have been predicted by considerations discussed in Chapter III. This may have been due to the temperature control limits being different than specified. Also the fact that the fluid heaters and temperature controller are physically separated in the gyroscope may allow wider temperature excursions of the damping fluid in the vicinity of the heaters or other fluid areas remote from the controller.

The compensation torque pulses used in Test 2 were applied at extremely unfavorable times. The chances of such pulse timing occurring in actual operation, except for short periods, are very remote. However, the chances of having a completely symmetrical distribution of torque pulses over the fluid temperature range is also remote. Therefore damping fluid temperature variations probably have some effect on digital drift compensation.

Test 3 - Test 3 shows that torque generator current transients can definitely affect digital drift compensation. The results of switching alternating input current when the steady-state current was at a relatively high value produced large drift rates. These drift rates were greatly reduced when the steady current wave was close to zero at the time of switching. The current pulses used for Test 3 were one cycle in width. Since the transients occur only on the ends of the pulses, as the pulse width is increased to a greater number of cycles the drift rate would be expected to be reduced by a factor of approximately the number of cycles. This proved to be the case in tests involving

larger numbers of cycles.

The results of using direct current pulses on the torque generator input winding shows that transients greatly affect the torque produced in such a case. As the pulse length was increased, decreasing the relative effects of the transients, the drift rates decreased almost proportionately. Unfortunately, when using direct current, there is no simple way of reducing the transients as there is for the alternating current case.

Test 4 - Torque generator residual magnetism caused by core material hysteresis effects produces residual torques when direct current excitation is used, as the results of Test 4 show. These residual torques cause drifting of the torque summing member and are definitely undesirable for digital drift compensation. Tests using alternating current on the torque generator windings showed no apparent residual torques caused by hysteresis effects.

Test 5 - The results of Test 5 indicate that the torque control methods used produce linear torque control and constant torques to a certain degree. This degree may be largely due to uncertainties in the measurements. The repeatability of the unbalance torques is somewhat in question. While the rotary table angle could be repeated with good accuracy, causes such as torque summing member mass shift due to bearing play and other uncertainties produced repeatability errors in the unbalance torques. The stability of the power supplies and other equipment used was also a factor. The drift torque rates observed may

have been of the order of magnitude of the uncertainty torques of the gyroscope used. Factors already mentioned such as suspension friction and damping fluid temperature changes may also have added to the drifts observed. The phase splitting transformer used did not produce exactly equal voltages on each side of the center tap. This is one reason the zero torque level as well as other torque levels of Method 2 produced drifts.

Since unbalance constants supplied with the gyroscope had an accuracy of only 0.1 meru, the results of Test 5 are probably as good as they need be for the compensation of the particular gyroscope used.

5.2 Conclusions

Drift compensation of a gyroscope with the use of digital information can be accomplished by several different methods. For many reasons these methods cannot cancel out the instantaneous error torque producing drift. They can, however, cancel out the long term effects of the error torque. The cancelling of these effects depends upon the integrating properties of the gyroscope. Thus digital controlled compensation differs from the normal method of drift compensation, which ideally can cancel out the instantaneous error torque and therefore does not rely heavily on integration by the gyroscope torque summing member. Certain factors cause the integration process in gyroscopes to be imperfect. Due to the extreme care used in making gyroscopes, these imperfections are quite small. They therefore do not appear to limit the usefulness of digital controlled drift compensation.

Some factors should receive special attention when drift compensation is digital controlled. They are as follows:

1. The maximum angular excursions of the torque summing member, caused by differences of the applied compensation torque from the ideal, should be less than the resolution of the gyroscope stabilization servo.

2. When digital accelerometers, such as the type discussed in Chapter III, are used to obtain the specific force data, the iteration time of the error torque digital computations depends upon the specific force profile to be experienced by the inertial system. If the system experiences frequent changes in specific force, the iteration time should be relatively short in order to reduce compensation torque quantization errors. If the system experiences infrequent changes in specific force, the iteration time should be relatively long in order to obtain more accurate specific force data.

3. The gyroscope damping fluid temperature should be maintained as constant as possible.

4. Only alternating currents should be used for the operation of the gyroscope torque generator. Switching transients and core material hysteresis effects cause direct current to be extremely undesirable for such use. In order to reduce transients, the alternating current should be switched only when the steady-state current wave passes through zero. To reduce the effects of any transients, the current pulses should contain only complete cycles and the shortest

pulse used should contain several cycles.

5. To reduce the effects of cross-coupling currents, the torque generator power supply should have a high output impedance.

5.3 Recommendations for Further Study

1. Work could be done on determining a method of calculating the error torque which would not necessitate a compromise in the iteration time for the desired results of low quantization error and high instantaneous torque determination accuracy.

2. A more accurate determination of the actual effects of the sources of error mentioned in Chapter III could be accomplished. This would probably require a more elaborate setup than was used for this thesis, utilizing better equipment and methods.

3. Work could be done on a method of digital torque control which operates by changing the phase angle between the torque generator excitation and input currents.

BIBLIOGRAPHY

1. Gianoukos, W. A., and Palmer, P. J., Gyro Test Laboratory Unbalance Equations, Report GT-130, MIT Instrumentation Laboratory, 1960.
2. Denhard, W. G., Laboratory Testing of a Floated, Single-Degree-of-Freedom, Integrating Inertial Gyro, Report R-105, MIT Instrumentation Laboratory, 1956.
3. Draper, C. S., Wrigley, W., and Grohe, L. R., The Floating Integrating Gyro and Its Application To Geometrical Stabilization Problems on Moving Bases, Institute of Aeronautical Sciences, 1955.
4. Gilinson, P. J., Jr., and Hofmann, G., Optimum Control of Instrument Output Axis Torque Inaccuracies, Report T-15, MIT Instrumentation Laboratory, 1952.
5. MIT Instrumentation Laboratory, The Spire, Jr. Long Range Inertial Guidance System, Report R-193, Final Engineering Report, 1959, SECRET.
6. Gauntt, F. E., Digitally Controlled Pulse Torquing of Precision Inertial Instruments, Report E-638, MIT Instrumentation Laboratory, 1957.
7. Cohen, A. R., A Design of a Practical Digital Accelerometer System, Master's Thesis, MIT Instrumentation Laboratory, 1958, CONFIDENTIAL.
8. Lees, Sidney, Integration by the Viscous Shear Process, Report 6398-T-10, MIT Instrumentation Laboratory, 1950.
9. Mueller, R. K., Microsyn Electromagnetic Components, MIT Instrumentation Laboratory, 1952.